



Synthesis, characterization, alkaline phosphatase inhibition assay and molecular modeling studies of 1-benzylidene-2-(4-tert-butylthiazol-2-yl) hydrazines

Hamid Aziz , Abid Mahmood , Sumera Zaib , Aamer Saeed , Hesham R. El-Seedi , Julie Pelletier , Jean Sévigny & Jamshed Iqbal

To cite this article: Hamid Aziz , Abid Mahmood , Sumera Zaib , Aamer Saeed , Hesham R. El-Seedi , Julie Pelletier , Jean Sévigny & Jamshed Iqbal (2020): Synthesis, characterization, alkaline phosphatase inhibition assay and molecular modeling studies of 1-benzylidene-2-(4-tert-butylthiazol-2-yl) hydrazines, Journal of Biomolecular Structure and Dynamics, DOI: [10.1080/07391102.2020.1802336](https://doi.org/10.1080/07391102.2020.1802336)

To link to this article: <https://doi.org/10.1080/07391102.2020.1802336>



View supplementary material [↗](#)



Published online: 11 Aug 2020.



Submit your article to this journal [↗](#)



Article views: 29




View related articles [↗](#)



View Crossmark data [↗](#)



Synthesis, characterization, alkaline phosphatase inhibition assay and molecular modeling studies of 1-benzylidene-2-(4-tert-butylthiazol-2-yl) hydrazines

Hamid Aziz^a, Abid Mahmood^b, Sumera Zaib^b, Aamer Saeed^a , Hesham R. El-Seedi^{c,d}, Julie Pelletier^e, Jean Sévigny^{e,f} and Jamshed Iqbal^b

^aDepartment of Chemistry, Quaid-I-Azam University, Islamabad, Pakistan; ^bCentre for Advanced Drug Research, COMSATS University Islamabad, Abbottabad Campus, Abbottabad, Pakistan; ^cInternational Research Center for Food Nutrition and Safety, Jiangsu University, Zhenjiang, China; ^dAl-Rayan Research and Innovation Center, Al-Rayan Colleges, Medina, Saudi Arabia; ^eCentre de Recherche du CHU de Québec, Université Laval, Québec, Canada; ^fDépartement de microbiologie-infectiologie et d'immunologie, Faculté de Médecine, Université Laval, Québec, Canada

Communicated by Ramaswamy H. Sarma

ABSTRACT

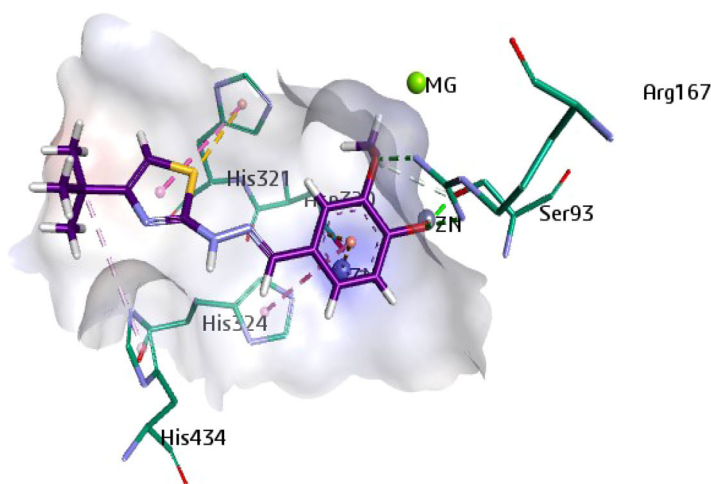
Alkaline phosphatases are homodimeric protein enzymes which removes phosphates from several types of molecules. These catalyze the hydrolysis of monoesters in phosphoric acid which in turn catalyze a transphosphorylation reaction. Thiazoles are a privileged class of heterocyclic compounds which may potentially serve as effective phosphatase inhibitors. In this regard, the present research paper reports the facile synthesis and characterization of substituted 1-benzylidene-2-(4-tert-butylthiazol-2-yl) hydrazines with excellent yields. The synthesized compounds were tested for inhibitory potential against alkaline phosphatases. The compound 1-(4-Hydroxy, 3-methoxybenzylidene)-2-(4-tert-butylthiazol-2-yl) hydrazine (**5e**) was found to be the most potent inhibitor of human tissue non-alkaline phosphatase in this group of molecules with an IC_{50} value of $1.09 \pm 0.18 \mu M$. The compound 1-(3,4-dimethoxybenzylidene)-2-(4-tert-butylthiazol-2-yl) hydrazine (**5d**) exhibited selectivity and potency for human intestinal alkaline phosphatase with an IC_{50} value of $0.71 \pm 0.02 \mu M$. In addition, structure activity relationship and molecular docking studies were performed to evaluate their binding modes with the target site of alkaline phosphatase. The docking analysis revealed that the most active inhibitors showed the important interactions within the binding pockets of human intestinal alkaline phosphatase and human tissue non-alkaline phosphatase and may be responsible for the inhibitory activity of the compound towards the enzymes. Therefore, the screened thiazole derivatives provided an outstanding platform for further development of alkaline phosphatase inhibitors.

ARTICLE HISTORY

Received 14 December 2019
Accepted 13 July 2020

KEYWORDS

Azomethine; alkaline phosphatase; molecular docking; radius of gyration; tissue non-specific; apo; holo



Alkaline phosphatase assay revealed compound **5e** (1-(4-Hydroxy, 3-methoxybenzylidene)-2-(4-tert-butylthiazol-2-yl) hydrazine) as the most active inhibitor of *h*-TNAP with an IC_{50} value of $1.09 \pm 0.18 \mu M$. Computational evaluation clearly depicts several interactions within the binding

pockets of ***h*-IAP** and ***h*-TNAP** and maybe responsible for the inhibitory potential of the compound towards the enzymes.

HIGHLIGHTS

- The synthesis of 1-(benzylidene) thiosemicarbazides **3(a-i)** was performed by reacting thiosemicarbazide with substituted aromatic aldehydes **1(a-i)**.
- The synthesized 1-(benzylidene) thiosemicarbazides was cyclized with 1-chloropinacolone to obtain the respective 1-benzylidene-2-(4-tert-butylthiazol-2-yl) hydrazines **5(a-i)**.
- The synthesized 1-benzylidene-2-(4-tert-butylthiazol-2-yl) hydrazines **5(a-i)** were successfully characterized using elemental analysis, FT-IR and multi nuclear NMR.
- Alkaline phosphatase assay and computational study was performed in favor of the synthesized 1-benzylidene-2-(4-tert-butylthiazol-2-yl) hydrazines **5(a-i)**.

Abbreviations: Anal: Analysis; APs: Alkaline Phosphatases; Arg150: Arginine 150; Arg167: Arginine 167; Asp316: Aspartate 316; Bio-assay: Biological Assay; Cald: Calculated; CDP-Star ®: Disodium 2-chloro-5-(4-methoxyspiro [1,2-dioxetane-3,2'-(5-chlorotricyclo[3.3.1.1^{3,7}] decan]-4-yl)-1-phenyl phosphate; CHN analyzer: Carbon Hydrogen and Nitrogen Analyzer; COS-7 cells: COS-7 cells; D: Doublet; DEA: Diethanolamine; DMEM: Dulbecco's Modified Eagle's Medium; DMF: Dimethylformamide; DMSO: Dimethyl sulfoxide; DNA: Deoxyribonucleic acid; EC: Enzyme Commission Number; FBS: Fetal Bovine Serum; FlexX: Name of program; FT-IR: Fourier-Transform Infrared Spectroscopy; ΔG: Gibbs free energy; GCAP: Germ Cells Alkaline Phosphatase; Glu108: Glutamate 108; Glu154: Glutamate 154; His317: Histidine 317; His320: Histidine 320; His321: Histidine 321; His324: Histidine 324; His358: Histidine 358; His432: Histidine 432; His434: Histidine 434; His437: Histidine 437; HYDE: Hydrogen bond and Dehydration Energies; *h*-IAP: Human Intestinal Alkaline Phosphatase; HIV-infections: Human Immunodeficiency Viruses-Infections; *h*-TNAP: Human Tissue Non-Specific Alkaline Phosphatase; IC₅₀: Half Maximal Inhibitory Concentration; IAP: Intestinal Alkaline Phosphatase; LTD₄ receptor antagonist: Leukotriene D₄ Receptor Antagonist; LeadIT: Name of software used for docking studies; MgCl₂: Magnesium Chloride; MHz: Mega Hertz; MMFF94x forcefield: Merck Molecular forcefield 94x; NMR: Nuclear Magnetic Resonance; MOE: Molecular Operating Environment; M.P.: Melting Point; Q: Quaternary; PLAP: Placental Alkaline phosphatase; Pro91: Proline 91; RCSB: Research Collaboratory for Structural Bioinformatics; R_f: Retention Factor; SD: Standard Deviation; SEM: Standard Error Mean; Ser92: Serine 92; Ser93: Serine 93; Singlet: Singlet; T: Triplet; Thr436: Threonine 436; tert-butyl: Tertiary-Butyl; TLC: Thin Layer Chromatography; TMS: Tetramethyl silane; TNAPs: Tissue Non-Specific Alkaline Phosphatases; Tyr169: Tyrosine 169; Tyr276: Tyrosine 276; Val90: Valine 90; ZnCl₂: Zinc chloride

1. Introduction

Alkaline phosphatases (**APs**, E.C. 3.1.3.1) are membrane bound homodimeric metallo-enzymes with an active site towards the extracellular space (Haarhaus et al., 2017). **APs** have five cysteine residues, two zinc atoms and one magnesium atom in each monomer. **APs** dephosphorylate phosphate mono-esters to ensure cellular events including protein phosphorylation, apoptosis and cellular growth at an alkaline pH (Millán, 2006). **APs** have four types of isozymes; germ cells (**GCAP**), tissue specific **APs** including placental (**PLAP**), intestinal (**IAP**) and tissue non-specific **APs** (**TNAPs**) (Sharma et al., 2014). **TNAPs** perform pyrophosphate hydrolysis to maintain an optimum pyrophosphate level in bone tissues. Intestinal **APs** regulate bicarbonate secretion, lipid intestinal absorption, detoxification of bacterial lipopolysaccharides and maintain pH values on the surface of duodenum (Al-Rashida et al., 2013). **APs** are overexpressed in tumor cells, including esophageal, breast, liver, intestinal, prostate, ovarian and intestinal cancer. ***h*-TNAP** and ***h*-IAP** level increases in cancer related therapies which turn them interesting molecular targets in drug design. As a result, there is an utmost demand in the synthesis of selective and effective inhibitors of **APs** isozymes. In this context, heterocyclic compounds such as 4-quinolones (Miliutina et al., 2017), coumarin-sulfonates (Salar et al., 2017), sulfonamides (Bhatti et al., 2017), triazoles, triazolothiadiazines and

triazolothiadiazoles offer attracting **APs** inhibitors. Some of the substituted thiazole analogues are investigated against **APs** and proven to be more potent inhibitors than the reference drug (Khan et al., 2014).

Thiazoles are five-membered aromatic heterocycles having nitrogen and sulfur atoms present at 1,3-positions of the ring (Ayati et al., 2015; Maradiya & Patel, 2003; Mishra et al., 2015). Thiazoles are copiously available in marine and terrestrial micro-organisms. These are also found in various naturally occurring and biologically significant molecules and are a prime component of thiamine (vitamin B₁) which is essential for the synthesis of acetylcholine to ensure normal functioning of the nervous system (Hutchinson et al., 2002). Thiazoles are potent inhibitors of stearyl coenzyme A delta-9 desaturase (Black et al., 2009), selective fatty acid amide hydrolase inhibitors (Wang et al., 2009), orexin receptor antagonist 2 (Bergman et al., 2006), amyloid-binding agents in neurodegenerative diseases (Henriksen et al., 2007), LTD₄ receptor antagonist (Lau et al., 1995) and histamine H₂ antagonists (Khanfar et al., 2016). Furthermore, thiazoles are novel therapeutic agents against hypertension, schizophrenia, thrombosis, inflammations and HIV-infections (Siddiqui et al., 2009) and effective agents for β-amyloid plaques, appetite depressants plant protectants (Gan et al., 2013) and photographic sensitizers (Keri et al., 2015). An extensive survey of literature reveals that the thiazole moiety can be incorporated as part of mono- or fused-rings, metal

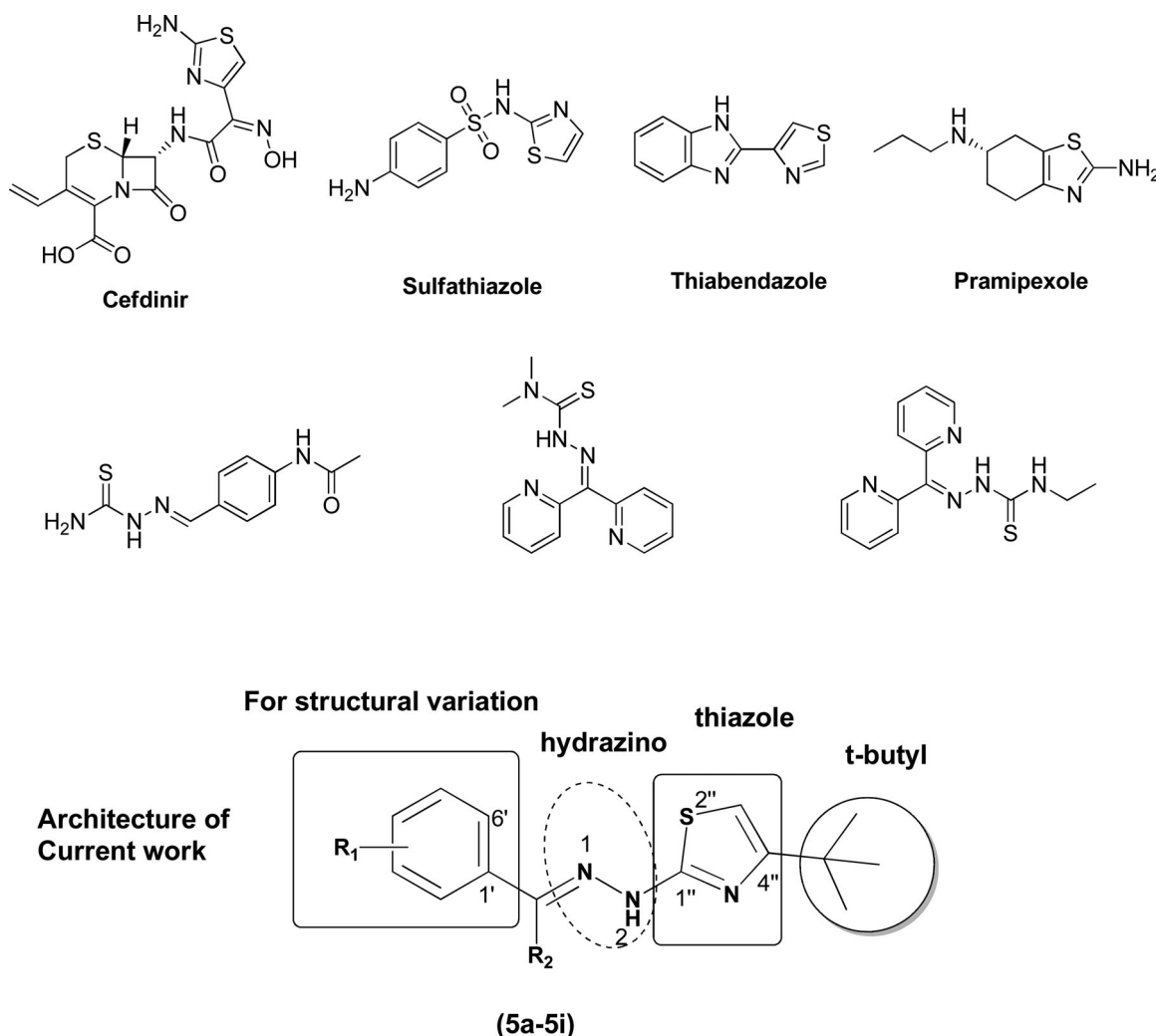


Figure 1. Some literature reported thiazole and thiosemicarbazones with significant biological activities.

complexes, and peptides while its removal causes the loss of the bioactivity. Thiazole ring is toxic to various cancer cell lines but nontoxic to normal cells and thus quite safer for human use (Chhabria et al., 2016; Ramos-Inza et al., 2019).

Conversely, hydrazino derivatives of 1,3-thiazole were reported to possess potent antimicrobial activities (Karegoudar et al., 2008). Hydrazino pharmacophores halt the synthesis of DNA and inhibit tumor cells. Triapine is a thiosemicarbazone derivative that has been reported as a potent anticancer drug. In addition, thiosemicarbazones based thiazoles demonstrate efficiency and lower toxicity profile as antimicrobials and antiproliferative agents (Braga et al., 2016). Figure 1 shows some thiazole derivatives with significant biological activities (Reddy & Reddy, 2010).

Thus, the addition of a hydrazine moiety further increases the biological potential of thiazoles. Consequently, in view of the potent profile of thiazoles on one hand and enhancement of biological potential by combination with hydrazine moiety on the other, we designed the target molecules possessing both structural features in a single moiety to prepare compounds as potential **APs** inhibitors.

The role of the *tert*-butyl structure in chemical, biocatalytic transformations and chemoenzymatic processes is well established (Bisel et al., 2008). The steric hindrance of a *tert*-

butyl group can either thwart a substrate from reacting or it can bring high selectivity in a reaction. It is one of the most popular groups in the synthesis of stable bioactive molecules with vividly better pharmacokinetic properties. For instance, the replacement of certain amino acid side chain by *tert*-butyl group increases the stability of peptides against chemical and enzymatic hydrolysis due to not only steric hindrance but also by considerably altering the secondary structures. The presence of *tert*-butyl group plays an important role in adjusting the lipophilicity and the solubility in biological systems.

The current research is related to the study of **APs** inhibition potential of some hydrazine linked thiazoles with *tert*-butyl group attachment. The synthesis was performed in a facile and efficient way in higher yields from commercially available aldehydes, thiosemicarbazide and 1-chloro-3,3-dimethylbutan-2-one.

2. Experimental

2.1. Chemistry

All the reagents employed in this research work were obtained from commercial sources and were used without

any further purification. The reactions were performed using oven dried glass ware at 70 °C for one hour under nitrogen atmosphere. ^1H and ^{13}C nuclear magnetic resonance (NMR) spectra were recorded on a Bruker spectrometer at 300 and 75 MHz, respectively. DMSO- d_6 was used as solvent and TMS was used as an internal reference. The ^1H -NMR data was reported as position (δ), relative integral, multiplicity (s, singlet; d, doublet; t, triplet; q, quaternary Carbon), coupling constant (J , Hz) and the assignment of the atom. The ^{13}C -NMR data were reported as position (δ) and assignment of the atom. Vertex 70 Bruker apparatus was used for recording the FT-IR spectra. The presence of each element was assessed from CHNS analyzer. Melting points were determined in a capillary tube using Stuart melting point apparatus (SMP3). The reaction progress was monitored through thin-layer chromatography on silica gel 60F254 with 0.25 mm (Merck) layer thickness.

2.2. Procedure for the synthesis of 1-(benzylidene) thiosemicarbazide 3(a-i)

The synthesis of 1-(benzylidene) thiosemicarbazides **3(a-i)** was achieved using our previously reported methodology (Saeed & Mumtaz, 2017). Briefly, appropriate aldehyde (1.0 mmol) was completely dissolved in dry ethanol (10 mL) by continuous stirring at room temperature. After half an hour, thiosemicarbazide (1.0 mmol) dissolved in dry ethanol (10 mL) was slowly added and the reaction mixture refluxed at 78 °C for 2 h. TLC was used to check the extent of completion of the reaction using *n*-hexane: ethyl acetate (4:1) solvent system. After 2 h, the reaction mixture was cooled and crushed ice was added which resulted in the formation of solid precipitates. The latter were filtered, dried and recrystallized from ethanol to afford pure 1-(benzylidene) thiosemicarbazides **3(a-i)**.

2.2.1. 1-(3-hydroxybenzylidene) thiosemicarbazide (3a)

M.P. 232–236 °C; R_f 0.32 (*n*-hexane: ethyl acetate, 4:1); Mol. wt: 195.24; (Yield 80%); IR (Pure, cm^{-1}) ν : 3379.43 (NH_2), 3289.16 (NH), 1620.43 ($\text{HC}=\text{N}$), 1598.84, 1556.20, 1479.60 ($\text{Ar}-\text{C}=\text{C}$), 1157.01 ($\text{C}=\text{S}$); ^1H NMR (300 MHz, DMSO- d_6 , δ): 10.23 (s, 1H, NH), 8.50 (s, 1H, OH), 8.23 (s, 1H, NH), 7.89 (s, 1H, NH), 8.45 (s, 1H, $\text{HC}=\text{N}$), 7.23 (d, 1H, $J=8.2$ Hz, $\text{Ar}-\text{H}$), 7.19 (s, 1H, $\text{Ar}-\text{H}$), 7.19 (t, 1H, $J=8.2$ Hz, $\text{Ar}-\text{H}$), 6.83 (d, 1H, $J=8.2$ Hz, $\text{Ar}-\text{H}$); ^{13}C NMR (75 MHz, DMSO- d_6 , δ): 181.43 ($\text{C}=\text{S}$), 158.90 (Ar), 143.30 ($\text{HC}=\text{N}$), 135.23 (Ar), 130.33 (Ar), 121.83 (Ar), 118.23 (Ar), 115.30 (Ar); Anal. Cald. For $\text{C}_8\text{H}_9\text{N}_3\text{OS}$: C, 49.21; H, 4.65; N, 21.52; S, 16.42; Found: C, 49.10; H, 4.75; N, 21.52; S, 16.40.

2.2.2. 1-(4-hydroxybenzylidene) thiosemicarbazide (3b)

M.P. 214–216 °C; R_f 0.37 (*n*-hexane: ethyl acetate, 4:1); Red powder; Mol. wt: 195.24; (Yield 82%); IR (Pure, cm^{-1}) ν : 3238.10 (NH_2), 3178.63 (NH), 1620.64 ($\text{HC}=\text{N}$), 1582.98, 1561.47, 1490.70 ($\text{Ar}-\text{C}=\text{C}$), 1159.67 ($\text{C}=\text{S}$); ^1H NMR (300 MHz, DMSO- d_6 , δ): 10.20 (s, 1H, NH), 8.45 (s, 1H, OH), 8.24 (s, 1H, NH), 7.90 (s, 1H, NH), 8.43 (s, 1H, $\text{HC}=\text{N}$), 7.43 (d,

2H, $J=7.52$ Hz, Ar), 6.83 (d, 2H, $J=7.52$ Hz, Ar); ^{13}C NMR (75 MHz, DMSO- d_6 , δ): 181.43 ($\text{C}=\text{S}$), 161.10 (Ar), 143.30 ($\text{HC}=\text{N}$), 130.90 (Ar), 126.43 (Ar), 116.30 (Ar); Anal. Cald. For $\text{C}_8\text{H}_9\text{N}_3\text{O}_3\text{S}$: C, 49.21; H, 4.65; N, 21.52; S, 16.42; Found: C, 49.12; H, 4.74; N, 21.42; S, 16.46.

2.2.3. 1-(5-bromo-2-hydroxybenzylidene) thiosemicarbazide (3c)

M.P. 236 °C; R_f 0.24 (*n*-hexane: ethyl acetate, 4:1); Brown powder; Mol. wt: 274.14; (Yield 78%); IR (Pure, cm^{-1}) ν : 3208.24 (NH_2), 3126.84 (NH), 2969.63 (sp^2 C-H), 1619.53 ($\text{HC}=\text{N}$), 1567.56, 1496.46 ($\text{Ar}-\text{C}=\text{C}$), 1240.98 ($\text{C}=\text{S}$); ^1H NMR (300 MHz, DMSO- d_6 , δ): 10.12 (s, 1H, NH), 8.40 (s, 1H, OH), 8.19 (s, 1H, NH), 7.84 (s, 1H, NH), 8.18 (s, 1H, $\text{HC}=\text{N}$), 7.63 (s, 1H), 7.39 (d, 1H, $J=8.2$ Hz, Ar), 6.73 (d, 1H, $J=8.2$ Hz, Ar); ^{13}C NMR (75 MHz, DMSO- d_6 , δ): 187.31 ($\text{C}=\text{S}$), 169.03 (Ar), 143.53 ($\text{HC}=\text{N}$), 135.13 (Ar), 133.90 (Ar), 124.80 (Ar), 122.48 (Ar), 118.30 (Ar); Anal. Cald. For $\text{C}_8\text{H}_8\text{BrN}_3\text{OS}$: C, 35.05; H, 2.94; N, 15.33; S, 11.70; Found: C, 35.05; H, 2.90; N, 15.30; S, 11.80.

2.2.4. 1-(3,4-dimethoxybenzylidene) thiosemicarbazide (3d)

M.P. 192–195 °C; R_f 0.22 (*n*-hexane: ethyl acetate, 4:1); Yellow powder; Mol. wt: 239.29; (Yield 75%); IR (Pure, cm^{-1}) ν : 3273.0 (NH_2), 3123.07 (NH), 2962.68 (sp^2 C-H), 2869.85 (sp^3 C-H), 1670.87 ($\text{HC}=\text{N}$), 1560.72, 1451.61 ($\text{Ar}-\text{C}=\text{C}$), 1234.02 ($\text{C}=\text{S}$); ^1H NMR (300 MHz, DMSO- d_6 , δ): 10.29 (s, 1H, NH), 8.36 (s, 1H, NH), 7.99 (s, 1H, NH), 7.89 (s, 1H, $\text{HC}=\text{N}$), 7.23 (s, 1H, $\text{Ar}-\text{H}$), 7.14 (d, 1H, $J=8.2$ Hz, $\text{Ar}-\text{H}$), 6.97 (d, 1H, $J=8.2$ Hz, $\text{Ar}-\text{H}$), 3.79 (s, 6H); ^{13}C NMR (75 MHz, DMSO- d_6 , δ): 179.08 ($\text{C}=\text{S}$), 148.32 (Ar), 146.40 (Ar), 139.91 ($\text{HC}=\text{N}$), 121.19 (Ar), 119.47 (Ar), 118.55 (Ar), 113.22 (Ar), 56.31 (O-C); Anal. Cald. For $\text{C}_{10}\text{H}_{13}\text{N}_3\text{O}_2\text{S}$: C, 50.19; H, 5.48; N, 17.56; S, 13.40; Found: C, 50.13; H, 5.58; N, 17.62; S, 13.40.

2.2.5. 1-(4-hydroxy-3-methoxybenzylidene) thiosemicarbazide (3e)

M.P. 222 °C; R_f 0.28 (*n*-hexane: ethyl acetate, 4:1); Orange powder; Mol. wt: 225.27; (Yield 73%); IR (Pure, cm^{-1}) ν : 3283.06 (NH_2), 3122.79 (NH), 3050.84 (sp^2 C-H), 2965.80 (sp^3 C-H), 1620.20 ($\text{HC}=\text{N}$), 1562.57, 1515.64, 1495.91 ($\text{Ar}-\text{C}=\text{C}$), 1154.32 ($\text{C}=\text{S}$); ^1H NMR (300 MHz, DMSO- d_6 , δ): 11.42 (s, 1H, NH), 9.19 (s, 1H, $\text{HC}=\text{N}$), 8.41 (s, 1H, OH), 8.12 (s, 1H, NH), 7.90 (s, 1H, NH), 7.53 (d, 1H, $J=7.80$ Hz, $\text{Ar}-\text{H}$), 6.93 (d, 1H, $J=7.80$ Hz, $\text{Ar}-\text{H}$), 6.75 (s, 1H), 3.79 (s, 3H, O-CH); ^{13}C NMR (75 MHz, DMSO- d_6 , δ): 178.08 ($\text{C}=\text{S}$), 148.32 (Ar), 146.40 (Ar), 139.91 ($\text{HC}=\text{N}$), 121.19 (Ar), 119.47 (Ar), 118.55 (Ar), 113.22 (Ar), 56.31 (O-C); Anal. Cald. For $\text{C}_9\text{H}_{11}\text{N}_3\text{O}_2\text{S}$: C, 47.99; H, 4.92; N, 18.65; S, 14.30; Found: C, 47.90; H, 4.95; N, 18.72; S, 14.10.

2.2.6. 1-(1-phenylethylidene) thiosemicarbazide (3f)

M.P. 132–134 °C; R_f 0.47 (*n*-hexane: ethyl acetate, 4:1); Light yellow powder; Mol. wt: 193.27; (Yield 81%); IR (Pure, cm^{-1}) ν : 3368.0 (NH_2), 3229.10 (NH), 3174.54 (sp^2 C-H), 2969.93 (sp^3 C-H), 1639.57 ($\text{C}=\text{N}$), 1578.56, 1548.86, 1499.54

(Ar-C=C), 1159.48 (C=S); ^1H NMR (300 MHz, DMSO- d_6 , δ): 10.21 (s, 1H, NH), 8.28 (s, 1H, NH), 7.94 (s, 1H, NH), 7.92 (m, 2H, Ar-H), 7.389 (m, 3H, Ar-H), 2.30 (s, 3H, C-H); ^{13}C NMR (75 MHz, DMSO- d_6 , δ): 179.36 (C=S), 148.28 (C=N), 138.11 (Ar), 129.66 (Ar), 128.69 (Ar), 127.06 (Ar), 14.46 (C-H); Anal. Cald. For $\text{C}_9\text{H}_{11}\text{N}_3\text{S}$: C, 55.93; H, 5.74; N, 21.74; S, 16.59; Found: C, 55.80; H, 5.82; N, 21.80; S, 16.62.

2.2.7. 1-(4-chlorobenzylidene) thiosemicarbazide (3g)

M.P. 210 °C; R_f = 0.19 (*n*-hexane: ethyl acetate, 4:1); Light yellow powder; Mol. wt: 213.69; (Yield 76%): IR (Pure, cm^{-1}) ν : 3180.38 (NH₂), 3106.65 (NH), 2962.165 (sp² C-H), 1596.64 (HC=N), 1575.19, 1519.73, 1489.17 (Ar-C=C), 1199.89 (C=S); ^1H NMR (300 MHz, DMSO- d_6 , δ): 10.26 (s, 1H, NH), 8.38 (s, 1H, NH), 7.89 (s, 1H, NH), 8.13 (s, 1H, HC=N), 7.69 (d, 2H, J = 8.10 Hz, Ar-H), 7.39 (d, 2H, J = 8.10 Hz, Ar-H); ^{13}C NMR (75 MHz, DMSO- d_6 , δ): 181.43 (C=S), 143.30 (HC=N), 136.63 (Ar), 131.93 (Ar), 130.63 (Ar), 129.13 (Ar); Anal. Cald. For $\text{C}_8\text{H}_8\text{ClN}_3\text{S}$: C, 44.97; H, 3.77; N, 19.66; S, 15.01; Found: C, 44.87; H, 3.81; N, 19.69; S, 15.1.

2.2.8. 1-(2,4-dihydroxybenzylidene) thiosemicarbazide (3h)

M.P. 245 °C; R_f = 0.18 (*n*-hexane: ethyl acetate, 4:1); Red powder; Mol. wt: 211.24; (Yield 68%): IR (Pure, cm^{-1}) ν : 3466.09 (NH₂), 3357.745 (NH), 3285 (OH), 3023.11, 2959.99 (sp² C-H), 1608.15 (HC=N), 1573.21, 1542.01, 1492.78 (Ar-C=C), 1202.47 (C=S); ^1H NMR (300 MHz, DMSO- d_6 , δ): 10.35 (s, 1H, NH), 8.32 (s, 1H, NH), 7.98 (s, 1H, NH), 8.13 (s, 1H, HC=N), 7.33 (d, 1H, J = 8.2 Hz, Ar-H), 6.39 (d, 1H, J = 8.2 Hz, Ar-H), 6.26 (s, 1H, Ar-H), 4.97 (s, OH); ^{13}C NMR (75 MHz, DMSO- d_6 , δ): 181.49 (C=S), 162.53 (Ar), 162.23 (Ar), 143.13 (HC=N), 132.13 (Ar), 111.13 (Ar), 108.63 (Ar), 103.73 (Ar); Anal. Cald. For $\text{C}_8\text{H}_9\text{N}_3\text{O}_2\text{S}$: C, 45.49; H, 4.29; N, 19.89; S, 15.18; Found: C, 45.43; H, 4.39; N, 19.96; S, 15.12.

2.2.9. 1-(furan-2-ylmethylene) thiosemicarbazide (3i)

M.P. 226–230 °C; R_f = 0.31 (*n*-hexane: ethyl acetate, 4:1); Light yellow powder; Mol. wt: 169.2; (Yield 70%): IR (Pure, cm^{-1}) ν : 3337.75 (NH₂), 3256.83 (NH), 2956.08 (sp² C-H), 1643.14 (HC=N), 1579.56, 1542.48, 1469.30 (Ar-C=C), 1134.54 (C=S); ^1H NMR (300 MHz, DMSO- d_6 , δ): 10.20 (s, 1H, NH), 8.18 (s, 1H, NH), 7.90 (s, 1H, NH), 7.53 (s, 1H, HC=N), 7.43 (d, 1H, J = 7.60 Hz, Ar-H), 6.36 (d, 1H, J = 7.60 Hz, Ar-H), 6.33 (t, 1H, J = 7.20 Hz, Ar-H); ^{13}C NMR (75 MHz, DMSO- d_6 , δ): 181.33 (C=S), 149.13 (Ar), 143.93 (Ar), 134.73 (HC=N), 109.93 (Ar), 109.53 (Ar); Anal. Cald. For $\text{C}_6\text{H}_7\text{N}_3\text{OS}$: C, 42.59; H, 4.17; N, 24.83; S, 18.95; Found: C, 42.50; H, 4.20; N, 24.85; S, 18.94.

2.3. Procedure for the synthesis of 1-benzylidene-2-(4-tert-butylthiazol-2-yl) hydrazine 5(a-i)

An equimolar mixture of 1-(benzylidene)thiosemicarbazides **3(a-i)** and 1-chloro-3,3-dimethylbutan-2-one (**4**) in dry ethanol was refluxed at 78 °C for 1.5 h. The completion of reaction was monitored by TLC was in *n*-hexane: ethyl acetate

(4:1) solvent system. The reaction mixture was concentrated under reduced pressure and poured onto crushed ice, the crude products obtained were recrystallized from ethanol at room temperature to afford the target 1-benzylidene-2-(4-tert-butylthiazol-2-yl) hydrazines **5(a-i)** (Saeed & Mumtaz, 2017).

2.3.1. 1-(3-hydroxybenzylidene)-2-(4-tert-butylthiazol-2-yl) hydrazine (5a)

M.P. 169 °C; R_f = 0.44 (*n*-hexane: ethyl acetate, 4:1); Red powder; Mol. wt: 275.37; (Yield 78%): IR (Pure, cm^{-1}) ν : 3300.54 (NH), 3117.26 (OH), 3044.77, 2967.92 (sp² C-H), 2903.53, 2868.53 (sp³ C-H), 1614.37 (HC=N), 1568.44, 1516.41, 1476.68 (Ar-C=C); ^1H NMR (300 MHz, DMSO- d_6 , δ): 11.08 (s, 1H, NH), 8.45 (s, 1H, HC=N), 7.40 (d, 1H, J = 8.2 Hz, Ar-H), 7.16 (s, 1H, Ar-H), 7.1 (t, 1H, J = 8.2 Hz, Ar-H), 6.9 (d, 1H, J = 8.2 Hz, Ar-H), 6.16 (s, 1H, C=C-H), 4.50 (s, 1H, OH), 1.39 (s, 9H, CH₃); ^{13}C NMR (75 MHz, DMSO- d_6 , δ): 172.13 (C=N), 162.13 (C=C), 159.22 (Ar), 143.55 (HC=N), 137.76 (Ar), 132.48 (Ar), 122.45 (Ar), 122.48 (Ar), 116.48 (Ar), 104.13 (thiazol-2-yl C=C), 39.13 (Cq), 32.13 (C-H); Anal. Cald. For $\text{C}_{14}\text{H}_{17}\text{N}_3\text{OS}$: C, 61.06; H, 6.22; N, 15.26; S, 11.64; Found: C, 61.06; H, 6.22; N, 15.24; S, 11.66.

2.3.2. 1-(4-hydroxybenzylidene)-2-(4-tert-butylthiazol-2-yl) hydrazine (5b)

M.P. 157 °C; R_f = 0.43 (*n*-hexane: ethyl acetate, 4:1); Red powder; Mol. wt: 275.37; (Yield 80%): IR (Pure, cm^{-1}) ν : 3173.20 (NH), 3115.33 (OH), 2966.49 (sp² C-H), 2867.97 (sp³ C-H), 1606.64 (HC=N), 1581.08, 1515.47, 1476.30 (Ar-C=C, aromatic); ^1H NMR (300 MHz, DMSO- d_6 , δ): 11.0 (s, 1H, NH), 8.45 (s, 1H, HC=N), 7.48 (d, 2H, J = 7.52 Hz, Ar-H), 6.89 (d, 2H, J = 7.52 Hz, Ar-H), 6.45 (s, 1H, C=C-H), 4.94 (s, 1H, OH), 1.45 (s, 9H, CH₃); ^{13}C NMR (75 MHz, DMSO- d_6 , δ): 171.83 (C=N), 161.21 (C=C), 160.41 (Ar), 142.15 (HC=N), 132.91 (Ar), 126.28 (Ar), 116.28 (Ar), 106.28 (thiazol-2-yl, C=C), 39.28 (Cq), 31.90 (C-H); Anal. Cald. For $\text{C}_{14}\text{H}_{17}\text{N}_3\text{OS}$: C, 61.06; H, 6.22; N, 15.26; S, 11.64; Found: C, 61.06; H, 6.24; N, 15.28; S, 11.60.

2.3.3. 1-(5-bromo-2-hydroxybenzylidene)-2-(4-tert-butylthiazol-2-yl) hydrazine (5c)

M.P. 180 °C; R_f = 0.36 (*n*-hexane: ethyl acetate, 4:1); Yellow powder; Mol. wt: 354.27; (Yield 75%): IR (Pure, cm^{-1}) ν : 3378.82 (NH), 3228.64 (OH), 3059.78 (sp² C-H), 2969.63 (sp³ C-H), 1619.53 (HC=N), 1567.56, 1496.46 (Ar-C=C); ^1H NMR (300 MHz, DMSO- d_6 , δ): 11.09 (s, 1H, NH), 8.18 (s, 1H, HC=N), 7.78 (s, 1H, Ar-H), 7.45 (d, 1H, J = 8.2 Hz, Ar-H), 7.25 (d, 1H, J = 8.2 Hz, Ar-H), 6.29 (s, 1H, C=C-H), 4.74 (s, 1H, OH), 1.45 (s, 9H, CH₃); ^{13}C NMR (75 MHz, DMSO- d_6 , δ): 170.45 (C=N), 162.34 (C=C), 159.34 (Ar), 145.23 (HC=N), 135.89 (Ar), 134.62 (Ar), 128.12 (Ar), 121.92 (Ar), 120.32 (Ar), 105.34 (thiazol-2-yl, C=C), 39.34 (Cq), 31.10 (C-H); Anal. Cald. For $\text{C}_{14}\text{H}_{16}\text{BrN}_3\text{OS}$: C, 47.46; H, 4.55; N, 11.86; S, 9.05; Found: C, 47.46; H, 4.55; N, 11.87; S, 9.10.

2.3.4. 1-(3,4-dimethoxybenzylidene)-2-(4-tert-butylthiazol-2-yl) hydrazine (5d)

M.P. 212 °C; R_f = 0.32 (*n*-hexane: ethyl acetate, 4:1); Red powder; Mol. wt: 319.42; (Yield 80%); IR (Pure, cm^{-1}) ν : 3153.85 (NH), 3000 (sp^2 C–H), 2959.60, 2866.80 (sp^3 C–H), 1609.72 (HC = N), 1569.01, 1524.01, 1456.78 (Ar–C = C); ^1H NMR (300 MHz, DMSO-d_6 , δ): 11.84 (s, 1H, NH), 7.99 (s, 1H, HC = N), 7.23 (s, 1H, Ar–H), 7.137 (d, 1H, J = 8.4 Hz, Ar–H), 6.975 (d, 1H, J = 8.4 Hz, Ar–H), 6.33 (s, 1H, C = C–H), 3.784 (s, 6H, OCH_3), 1.22 (s, 9H, CH_3); ^{13}C NMR (75 MHz, DMSO-d_6 , δ): 168.36 (C = N), 162.07 (C = C), 150.36 (Ar), 149.43 (Ar), 141.22 (HC = N), 127.89 (Ar), 120.39 (Ar), 112.12 (Ar), 108.81 (Ar), 99.78 (thiazol-2-yl, C = C), 55.98, 55.79 (O–C), 34.73 (Cq), 33.03 (C–H); Anal. Cald. For $\text{C}_{16}\text{H}_{21}\text{N}_3\text{O}_2\text{S}$: C, 60.16; H, 6.63; N, 13.16; S, 10.04; Found: C, 60.10; H, 6.60; N, 13.15; S, 10.14.

2.3.5. 1-(4-hydroxy, 3-methoxybenzylidene)-2-(4-tert-butylthiazol-2-yl) hydrazine (5e)

M.P. 145 °C; R_f = 0.30 (*n*-hexane: ethyl acetate, 4:1); Red powder; Mol. wt: 305.4; (Yield 74%); IR (Pure, cm^{-1}) ν : 3216.75 (NH), 314.81 (OH), 3059.29, 2955.35 (sp^2 C–H), 2913.07 (sp^3 C–H), 1672.72 (HC = N), 1567.26, 1419.61 (Ar–C = C); ^1H NMR (300 MHz, DMSO-d_6 , δ): 11.09 (s, 1H, NH), 8.20 (s, 1H, HC = N), 7.23 (d, 1H, J = 8.02 Hz, Ar–H), 7.05 (s, 1H, Ar–H), 7.0 (d, 1H, J = 8.02 Hz, Ar–H), 6.20 (s, 1H, C = C–H), 3.74 (s, 3H, O–CH), 5.01 (s, 1H, OH), 1.41 (s, 9H, CH_3); ^{13}C NMR (DMSO- d_6 , 75 MHz) δ : 172.53 (C = N), 162.53 (C = C), 152.34 (Ar), 150.23 (Ar), 143.89 (HC = N), 128.12 (Ar), 122.92 (Ar), 118.32 (Ar), 114.89 (Ar), 104.53 (thiazol-2-yl, C = C), 56.89 (O–C), 40.13 (Cq), 32.53 (C–H); Anal. Cald. For $\text{C}_{15}\text{H}_{19}\text{N}_3\text{O}_2\text{S}$: C, 58.99; H, 6.27; N, 13.76; S, 10.50; Found: C, 58.99; H, 6.29; N, 13.77; S, 10.53.

2.3.6. 1-(4-tert-butylthiazol-2-yl)-2-(1-phenylethylidene) hydrazine (5f)

M.P. 140 °C; R_f = 0.59 (*n*-hexane: ethyl acetate, 4:1); Black powder; Mol. wt: 273.4; (Yield 80%); IR (Pure, cm^{-1}) ν : 3149.61 (NH), 3000, 2913.07 (sp^2 C–H), 2954.04, 2855.35 (sp^3 C–H), 1676.0 (C = N), 1567.26, 1419.61 (Ar–C = C); ^1H NMR (300 MHz, DMSO-d_6 , δ): 11.09 (s, 1H, NH), 7.63 (d, 2H, J = 8.02 Hz, Ar–H), 7.35 (t, 2H, J = 8.02 Hz, Ar–H), 7.25 (t, 1H, J = 8.02 Hz, Ar–H), 6.20 (s, 1H, C = C–H), 1.41 (s, 9H, CH_3), 0.90 (s, 3H, CH_3); ^{13}C NMR (75 MHz, DMSO-d_6 , δ): 171.53 (C = C), 168.89 (C = N), 162.89 (C = N), 136.34 (Ar), 132.23 (Ar), 129.12 (Ar), 127.92 (Ar), 100.20 (thiazol-2-yl, C = C), 40.13 (Cq), 32.53 (C–H), 20.89 (C–H); Anal. Cald. For $\text{C}_{15}\text{H}_{19}\text{N}_3\text{S}$: C, 65.90; H, 7.00; N, 15.37; S, 11.73; Found: C, 65.90; H, 7.00; N, 15.40; S, 11.70.

2.3.7. 1-(4-chlorobenzylidene)-2-(4-tert-butylthiazol-2-yl) hydrazine (5g)

M.P. 165 °C; R_f = 0.30 (*n*-hexane: ethyl acetate, 4:1); Yellow powder; Mol. wt: 293.81; (Yield 70%); IR (Pure, cm^{-1}) ν : 3183.93 (NH), 2962.98 (sp^2 C–H), 2923.656.37 (sp^3 C–H), 1597.61 (HC = N), 1576.38, 1520.99, 1490.14 (Ar–C = C); ^1H NMR (400 MHz, DMSO-d_6 , δ): 11.09 (s, 1H, NH), 7.68 (s, 1H,

HC = N), 7.57 (d, 2H, J = 8.40 Hz, Ar–H), 7.34 (d, 2H, J = 8.40 Hz, Ar–H), 6.25 (s, 1H, C = C–H), 1.28 (s, 9H, CH_3); ^{13}C NMR (100 MHz, DMSO-d_6 , δ): 167.49 (C = N), 161.95 (C = C), 139.73 (HC = N), 135.16 (Ar), 132.74 (Ar), 128.96 (Ar), 127.82 (Ar), 100.81 (thiazol-2-yl, C = C), 34.56 (Cq), 29.71 (C–H); Anal. Cald. For $\text{C}_{14}\text{H}_{16}\text{ClN}_3\text{S}$: C, 57.23; H, 5.49; N, 14.30; S, 10.91; Found: C, 57.21; H, 5.49; N, 14.30; S, 10.93.

2.3.8. 1-(2,4-dihydroxybenzylidene)-2-(4-tert-butylthiazol-2-yl) hydrazine (5h)

M.P. 125 °C; R_f = 0.34 (*n*-hexane: ethyl acetate, 4:1); Red powder; Mol. wt: 291.37; (Yield 78%); IR (Pure, cm^{-1}) ν : 3122.09 (NH), 3023.11 (OH), 3959.59 (sp^2 C–H), 2864.51 (sp^3 C–H), 1608.15 (HC = N), 1573.21, 1542.01, 1445.35 (Ar–C = C); ^1H NMR (300 MHz, DMSO-d_6 , δ): 11.09 (s, 1H, NH), 7.85 (s, 1H, HC = N), 7.30 (d, 1H, J = 8.20 Hz, Ar–H), 7.15 (d, 1H, J = 8.20 Hz, Ar–H), 7.0 (s, 1H, Ar–H), 4.50 (s, 2H, OH), 1.33 (s, 9H, CH_3); ^{13}C NMR (75 MHz, DMSO-d_6 , δ): 170.23 (C = N), 161.89 (C = C), 164.89 (Ar), 163.34 (Ar), 143.13 (HC = N), 132.13 (Ar), 112.12 (Ar), 109.89 (Ar), 104.89 (Ar), 104.56 (thiazol-2-yl, C = C), 39.23 (Cq), 31.56 (C–H); Anal. Cald. For $\text{C}_{14}\text{H}_{17}\text{N}_3\text{O}_2\text{S}$: C, 57.71; H, 5.88; N, 14.42; S, 11.00; Found: C, 57.69; H, 5.83; N, 14.38; S, 11.10.

2.3.9. 1-(4-tert-butylthiazol-2-yl)-2-(furan-2-ylmethylene)-hydrazine (5i)

R_f = 0.35 (*n*-hexane: ethyl acetate, 4:1); Viscous liquid; Mol. wt: 249.33; (Yield 80%); IR (Pure, cm^{-1}) ν : 3267.53 (NH), 3014.11 (sp^2 C–H), 2954.04, 2855.35 (sp^3 C–H), 1678.22 (HC = N), 1567.26, 1419.61 (Ar–C = C); ^1H NMR (300 MHz, DMSO-d_6 , δ): 11.09 (s, 1H, NH), 7.85 (s, 1H, HC = N), 7.30 (d, 1H, J = 8.02 Hz, Ar–H), 7.06 (d, 1H, J = 7.60 Hz, Ar–H), 7.0 (t, 1H, J = 7.60 Hz, Ar–H), 6.33 (s, 1H, J = 7.22 Hz, Ar–H); 1.35 (s, 9H, CH_3); ^{13}C NMR (75 MHz, DMSO-d_6 , δ): 171.23 (C = N), 161.33 (C = C), 150.89 (Ar), 144.34 (Ar), 143.13 (HC = N), 112.13 (Ar), 111.12 (Ar), 39.63 (Cq), 31.96 (C–H); Anal. Cald. For $\text{C}_{12}\text{H}_{15}\text{N}_3\text{OS}$: C, 57.81; H, 6.06; N, 16.85; S, 12.86; Found: C, 57.83; H, 6.06; N, 16.87; S, 12.82.

2.4. Bioassays

2.4.1. Cell transfection

Plasmids encoding the **h-TNAP** and **h-IAP** were transfected as reported previously (Kukulski et al., 2005). COS-7 cells were seeded 24 h before transfection as cells gained the confluency of 80–90%. COS-7 cells were incubated for 5–6 h at 37 °C in 5% CO_2 incubator after adding serum free dulbecco's modified eagle's medium (DMEM) containing 6 μg of plasmid DNA and 24 μL of lipofectamine reagent. After 48 h, serum free medium was replaced with cell culture medium containing 20% fetal bovine serum (FBS). Expressed proteins were extracted and quantify by Bradford method (Bradford, 1976). Aliquots of protein fraction were made with 7.5% glycerol and stored at -80°C .

2.4.2. Alkaline phosphatase inhibition assay

The synthesized compounds **5(a-i)** were analyzed for enzyme inhibitory activity on recombinant **h-TNAP** and **h-IAP** after slight changes in the previously reported method (Sergienko & Millán, 2010). Disodium 2-chloro-5-(4-methoxyspiro [1,2-dioxetane-3,2'-(5-chlorotricyclo[3.3.1.1.3.7] decan]) 4-yl]-1-phenyl phosphate, also known as CDP-Star®, was used as a chemoluminescent substrate in enzyme inhibitory assay. Working solution of **h-TNAP** (5 µg/mL) and **h-IAP** (3.335 µg/mL) were prepared in dilution buffer containing diethanolamine (DEA) 250 mM, ZnCl₂ 0.05 mM and MgCl₂ 2.5 mM. Assay was performed by adding 20 µL enzyme solution, 10 µL of test compound (final compound concentration 200 µM and DMSO conc. less than 2% v/v) in 384 wells white plate. After an incubation of 5 to 7 min, luminescence signals were taken by microplate reader (BioTek FLx800, Instruments, Inc. USA). To each well, 20 µL of CDP-Star® was added with final concentration of 105.2 µM and 177 µM for **h-TNAP** and **h-IAP**, respectively. After an incubation of 7–10 min, after-read was taken by measuring luminescence signals. Percentage of inhibition was measured for each compound, and those exhibited an inhibition more 50% were further analyzed for IC₅₀ value measurement. Data was analyzed by using PRISM 5.0 (GraphPad, San Diego, California, USA) software.

2.4.3. Molecular docking and dynamic simulation studies

To justify the inhibition caused by potent inhibitors, most plausible binding modes were predicted using molecular docking studies. Because of unavailability of x-ray crystallographic structure of human alkaline phosphatases, homology models generated previously by our research group were used for docking studies (Ausekle et al., 2016). Structures of the tested compounds were drawn by MOE builder tool (MOE, 2016) and optimization was achieved using MMFF94x forcefield (Labute, 2007). Afterwards the energy minimization of the target proteins was carried out by Molecular Operating Environment (Schneider et al., 2013). LeadIT (BioSolveIT GmbH, Germany) (LeadIT, 2017) was used to perform docking analysis of the prepared ligands inside the respective receptors. Load Receptor Utility of the LeadIT software was used to load the receptor and the metallic ions were selected as part of the protein. Active pocket of the protein for docking analysis was identified by keeping the amino acid residues in 9.0 Å radius around catalytic zinc ions and magnesium ion. Values of the amino acid flips, metal co-ordinates and water handling were kept as by default. Once docking analysis was completed, the possible interactions of ligands with receptor proteins were inspected for studying the possible interactions using HYDE assessment (Schneider et al., 2013). Discovery Studio Visualizer was used to perform visualize the interactions of ligand and receptors (Dassault Systèmes Biovia, 2016).

For MD simulations, protein manipulation and protonation were made with the help of GROMOS96 force field having the 43a1 parameter set. The GROMACS simulation packages, 5.1.4 were used for the MD simulations using previously used methods (Ferreira et al., 2012; Mathew et al., 2016; Özgeriş et al., 2016). Parametrization of the selected compound was carried out by online PRODRG servers (Schüttelkopf & van Aalten,

2004). VMD (Humphrey et al., 1996) was used for the visualization of trajectories. After the energy minimization of system, two sequential NVT (100 ps) and NPT (100 ps) runs were performed for equilibration of system. The resulting ensembles were subjected to 20 ns MD simulations with a time step of 2 fs. Periodic boundary conditions were applied during MD simulations. All NVT and NPT ensembles used the Berendsen thermostat and the Parrinello-Rahman barostat for temperature (approx. 302–303 K) and pressure coupling (approx. 1.01 bar), respectively. Cut-off radii of 10 Å and smooth Particle Mesh Ewald protocol were observed for long-range method. Root mean square deviation of protein was plotted using XMGRACE v5.1.19 (Turner, 2005).

3. Results and discussion

3.1. Synthesis of 1-benzylidene-2-(4-tert-butylthiazol-2-yl) hydrazine **5(a-i)**

The synthetic route adopted for the synthesis of 1-benzylidene-2-(4-tert-butylthiazol-2-yl) hydrazine derivatives **5(a-i)** is presented in Figure 2. The synthesis was carried out in two steps. In the first step, suitably substituted aromatic aldehydes **1(a-i)** were reacted with thiosemicarbazide (**2**) in dry ethanol at reflux temperatures of 78 °C for 2 h using catalytic amount of concentrated sulphuric acid. After the reaction was completed, the mixture was gradually cooled to room temperature and poured onto crushed ice resulting in solid precipitates. The latter were filtered, dried and recrystallized from ethanol to furnish pure 1-(benzylidene) thiosemicarbazides **3(a-i)** in good yields (68–83%). In the second step, the key intermediates **3(a-i)** were treated with 1-chloro-3,3-dimethylbutan-2-one (**4**) in ethanol at reflux temperature of 78 °C for 1.5 h. The reaction was constantly monitored by thin layer chromatography in a solvent system of *n*-hexane: ethyl acetate 4:1. On completion, the solvent was rotary evaporated, and the reaction mixture was poured onto ice cold water followed by recrystallization from ethanol to obtain the target 1-benzylidene-2-(4-tert-butylthiazol-2-yl) hydrazine **5(a-i)** in excellent (84–70%) yields (Table 1).

3.2. Characterization

The structural confirmation of the small library of the synthesized compounds (**3a-5i**) was performed through microelemental (CHNS), and spectroscopic analysis including FT-IR, ¹H NMR and ¹³C NMR. Accordingly, elemental analyzer provided data highly aligned with the elements present in the synthesized compounds (**3a-5i**). ¹H NMR spectra of 1-(benzylidene) thiosemicarbazides **3(a-i)** displayed signals in the range of 11.42–7.84 ppm for NH and NH₂ protons respectively. The characteristic peak for azomethine carbon of 1-(benzylidene)thiosemicarbazide derivatives **3(a-i)** displayed sharp singlet at 7.53–9.19 and 134.13–143.53 ppm in ¹H NMR and ¹³C NMR respectively. The thiocarbonyl (C=S) functional group displayed marked appearance in the range of 178.08–187.31 ppm in ¹³C NMR. The target 1-benzylidene-2-(4-tert-butylthiazol-2-yl) hydrazine derivatives **5(a-i)** displayed

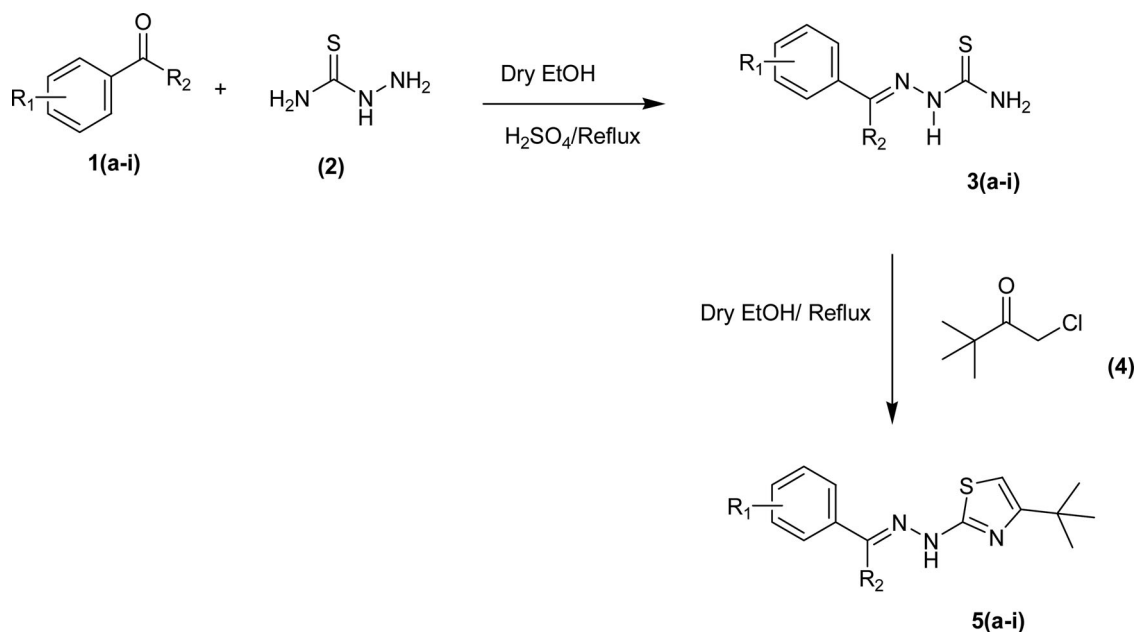


Figure 2. Synthesis of 1-benzylidene-2-(4-tert-butylthiazol-2-yl) hydrazine derivatives (3a-5i).

Table 1. The variously substituted synthesized 1-benzylidene-2-(4-tert-butylthiazol-2-yl) hydrazine derivatives (3a-5i).

S.No.	Compound	R ₁	R ₂	S.No.	Compound	R ₁	R ₂
1	3a	3-OH	H	10	5a	3-OH	H
2	3b	4-OH	H	11	5b	4-OH	H
3	3c	2-OH, 5-Br	H	12	5c	2-OH, 5-Br	H
4	3d	3,4-di-OCH ₃	H	13	5d	3,4-di-OCH ₃	H
5	3e	3-OCH ₃ , 4-OH	H	14	5e	3-OCH ₃ , 4-OH	H
6	3f	H	CH ₃	15	5f	H	CH ₃
7	3g	4-Cl	H	16	5g	4-Cl	H
8	3h	2,4-di-OH	H	17	5h	2,4-di-OH	H
9	3i	2-thiophene	H	18	5i	2-thiophene	H

sharp signal for sp^2 hybridized thiazole carbon in the range of 99.78–106.40 ppm and for attached proton in the range of 6.16–6.45 ppm in ^{13}C NMR and ^1H NMR respectively. The nine-proton singlet for the tert-butyl group appeared around 1.22–1.45 ppm in ^1H NMR whilst the quaternary and methyl carbons made appearance at in the range of 34.56–40.63 and 29.13–33.03 ppm in ^{13}C NMR.

3.3. Biological activities

3.3.1. Structure activity relationship (SAR)

The synthesized compounds **5(a-i)** were analyzed for their inhibitory potential on tissue specific **APs** as well as human tissue non-specific alkaline phosphatase (**h-TNAP**) enzymes as structural features of these compounds exhibited resemblance to the already reported inhibitors of alkaline phosphatase. Levamisole (6-phenyl-2,3,5,6-tetrahydroimidazo[2,1-b][1,3]thiazole) is a well-known inhibitor of alkaline phosphatase. Structural features of levamisole signify the role of thiazole moiety in alkaline phosphatase inhibition (Chang et al., 2011). Tertiary butyl group fused with aromatic structures confer the inhibitory potential for alkaline phosphatase (Iqbal et al., 2018). Hydrazine derivatives are known to inhibit alkaline phosphatase as well as acid phosphatase. Among various synthesized hydrazine derivatives 2-(4,6-Dimethylpyrimidin-2-

yl)-1-[1-(6-nitrobenzaldehyde)ethylidene]hydrazine was found to be more potent against both the clinically significant enzymes (Ravish & Raghav, 2016). Both isozymes were human recombinant enzymes. Human intestinal **APs** (**h-IAP**) was taken as tissue specific **APs** to assess the selective inhibitory potential of the synthesized compounds. The obtained results showed that all the tested compounds were active inhibitors against both the isozymes. However, some of the tested compounds exhibited selective potential against **h-IAP**. The tested compounds **5a**, **5b**, **5e**, **5g** were found to be potent as well as non-selectivity for both the isozymes and compound **5d** and **5h** were selective for **h-IAP**. Among the tested compounds, **5e** is more potent with an IC_{50} value of $1.09 \pm 0.18 \mu\text{M}$ for **h-TNAP**. Benzyl of compound **5e** possess hydroxyl group at *p*-position with adjacent methoxy moiety which is 23 folds more potent as compared to known inhibitor of **h-TNAP**, levamisole ($\text{IC}_{50} = 25.2 \pm 1.90 \mu\text{M}$). Replacement of benzyl group with furan ring (**5i**) confers the selectivity towards **h-TNAP** having IC_{50} value of $3.49 \pm 0.14 \mu\text{M}$. Synthesized derivative **5d** with adjacent methoxy groups at benzyl ring exhibited selectivity and potency against **h-IAP** having an IC_{50} value of $0.71 \pm 0.02 \mu\text{M}$. Structural data represents that un-substituted (**5f**) as well as bromine substituted (**5c**) benzyl derivatives were not too potent against both the isozymes and exhibited inhibitory potential less than 50% (Table 2).

3.3.2. Enzyme kinetics study for h-TNAP and h-IAP inhibition

Enzyme kinetics studies were carried out to find the mode of enzyme inhibition of most potent and selective compounds for **h-TNAP** and **h-IAP**. **5e** exhibited competitive and uncompetitive mode of inhibition for **h-TNAP** and **h-IAP** respectively, whereas, **5d** was found to possess non-competitive mode of inhibition (Figure 3).

3.3.3. Molecular modeling investigation and molecular simulation simulations

For further detailed insight into the activities of the synthesized compounds **5(a-i)** for human alkaline phosphatases (**h-IAP** and **h-TNAP**), molecular modeling was performed for selective and most active analogues. LeadIT software was used for carrying out the modeling analysis of selected compounds (LeadIT, 2017). The crystal structures of the target proteins were unavailable at RCSB protein databank, hence previously reported homology models were used (Ausekle et al., 2016).

Levamisole ((S)-6-phenyl-2,3,5,6-tetrahydroimidazo[2,1-b]thiazole) used as positive control in the biological assay was docked inside the binding site of tissue non-specific **APs** (Figure 4(c)). The resultant interactions involve conventional hydrogen bonding (1.86 Å) by nitrogen of imidazole ring with His437 and π -alkyl linkage of the same residue (3.85 Å) with thiazole ring. Val90 was at alkyl linkage (4.61 Å) with the thiazole ring. Three additional carbon H-bonds were noticed by Glu108 (2.60 Å), Pro91 (2.76 Å) and Thr436 (2.45 Å). Compound **5e**, the most active inhibitor exhibited several interactions within the binding pocket of **h-TNAP** as represented in Figure 4(a). Hydrogen bonds were formed by Arg167 with methoxy (2.56 Å) and hydroxyl group (2.46 Å) of 2-methoxyphenol. However, Ser93 showed a conventional H-bond (1.54 Å) with hydroxyl group and a carbon H-bond (2.74 Å) with methoxy group. Two π - π T-shaped interactions were examined by thiazole ring with His324 (4.74 Å) and phenol ring with His321 (4.91 Å). Additionally, a π -sulfur linkage was shown by His321 (3.66 Å) with sulfur of thiazole ring. His434 shown π -alkyl linkage (5.42 Å) with 4-tert-butyl moiety of thiazole ring. A π -cation (2.81 Å) linkage was made with Zn ion. The interactions of levamisole are similar to those exhibited by potent compound. The results are in

accordance with the previously shown interactions within the active pocket of **h-TNAP** (Andleeb et al., 2019; Ausekle et al., 2016; Khan et al., 2015). Compound **5b** (dual inhibitor of both the isozymes) was docked within the binding site of **h-TNAP** (Figure 4(b)) and the most notable interactions were hydrogen bonding of phenol ring (hydroxyl group) with Arg167 (2.63 Å) and Ser93 (1.66 Å). π - π T-shaped interactions were formed by phenol ring with His437 (5.17 Å) and His154 (5.96 Å), while, thiazole ring with His321 (5.33 Å). In addition, π -alkyl linkage was formed by 4-tert-butyl moiety of thiazole ring with His434 (5.38 Å) and a π -sulfur linkage was observed by sulfur of thiazole ring with His321 (4.05 Å). All the interactions with the amino acid residues of active pocket are similar to important interactions reported previously (Khan et al., 2015; Salar et al., 2017). The docking analysis revealed that the most active inhibitor exhibits the important interactions within the binding pocket of **h-TNAP** and maybe responsible for the inhibitory activity of the compound towards the enzyme.

Molecular docking analysis of L-phenylalanine inside the binding pocket of human intestinal alkaline phosphatase revealed that π - π stacked interactions were shown by phenyl ring with His320 (4.32 Å) and π - π T-shaped with His432 (5.55 Å). His358 showed a hydrogen bond (2.77 Å) and a carbon H bond (2.18 Å) with phenylalanine. Amino acid Ser92 made a hydrogen bond (2.16 Å) with oxygen of the alanine group and the same oxygen was involved in a metal acceptor interaction with zinc (2.39 Å). Compound **5d** (the most active inhibitor of **h-IAP**) exhibited extensive network of hydrogen bonds like hydrazine showed H bond with Glu321 (1.82 Å), methoxy group with Tyr276 (2.72 Å), sulfur of thiazole ring with Arg314 (3.34 Å), nitrogen atom of hydrazine with Arg314 (2.69 Å) and methoxy group of benzylidene with Arg314 (2.98 Å). Additionally, His317 formed π - π stacked interaction with thiazole (3.86 Å) and π -sulfur interactions with sulfur within the same ring (4.05 Å). Compound **5b** (dual inhibitor) formed π - π T-shaped interactions with His320 (5.19 Å) by phenol ring and Tyr169 (5.39 Å) by thiazole ring. Furthermore, hydrogen bonds were observed between Asp316 (2.81 Å) and hydroxyl group of phenol ring, Arg150 (2.71 Å) and nitrogen atom of thiazole ring, Tyr169 (2.02 Å) and nitrogen atom of hydrazine moiety. Tyr169 also showed a π -sulfur linkage (5.61 Å) with the compound **5b**. Moreover, a metal acceptor interaction was observed with zinc. The mode of orientation and the binding interactions are in agreement with reported binding of active compounds

Table 2. Inhibitory potential of 1-benzylidene-2-(4-tert-butylthiazol-2-yl) hydrazine **5(a-i)** for alkaline phosphatase isozymes.

Compound	<i>h</i> -TNAP IC ₅₀ ± SEM (μM) / % inhibition ± SD	<i>h</i> -IAP IC ₅₀ ± SEM (μM) / % inhibition ± SD
5a	27.3 ± 3.24	8.50 ± 0.09
5b	4.88 ± 0.30	5.47 ± 0.75
5c	25 ± 2%	43 ± 1%
5d	41 ± 2%	0.71 ± 0.02
5e	1.09 ± 0.18	6.51 ± 0.35
5f	28 ± 2%	32 ± 1%
5g	6.02 ± 0.13	2.12 ± 0.24
5h	28 ± 2%	8.80 ± 0.26
5i	3.49 ± 0.14	41 ± 3%
Levamisole	25.2 ± 1.90	—
L-phenylalanine	—	100 ± 3.00

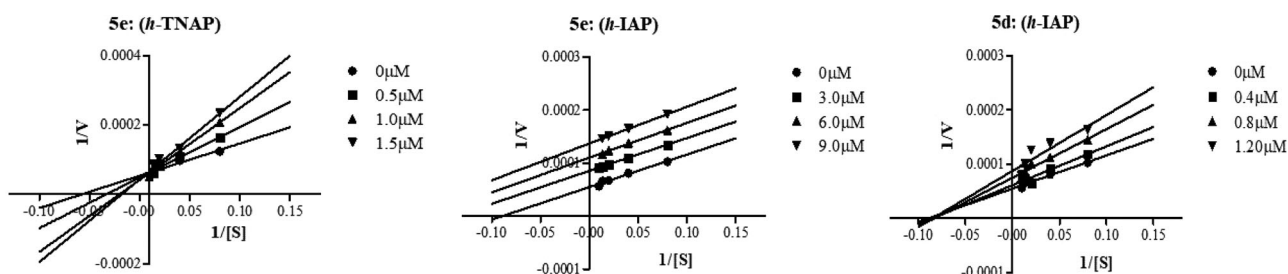


Figure 3. Double reciprocal plot of enzyme kinetics of **h-TNAP** for **5e** (right) and **h-IAP** for **5e** (middle), **5d** (left) describing the mode of enzyme inhibition.

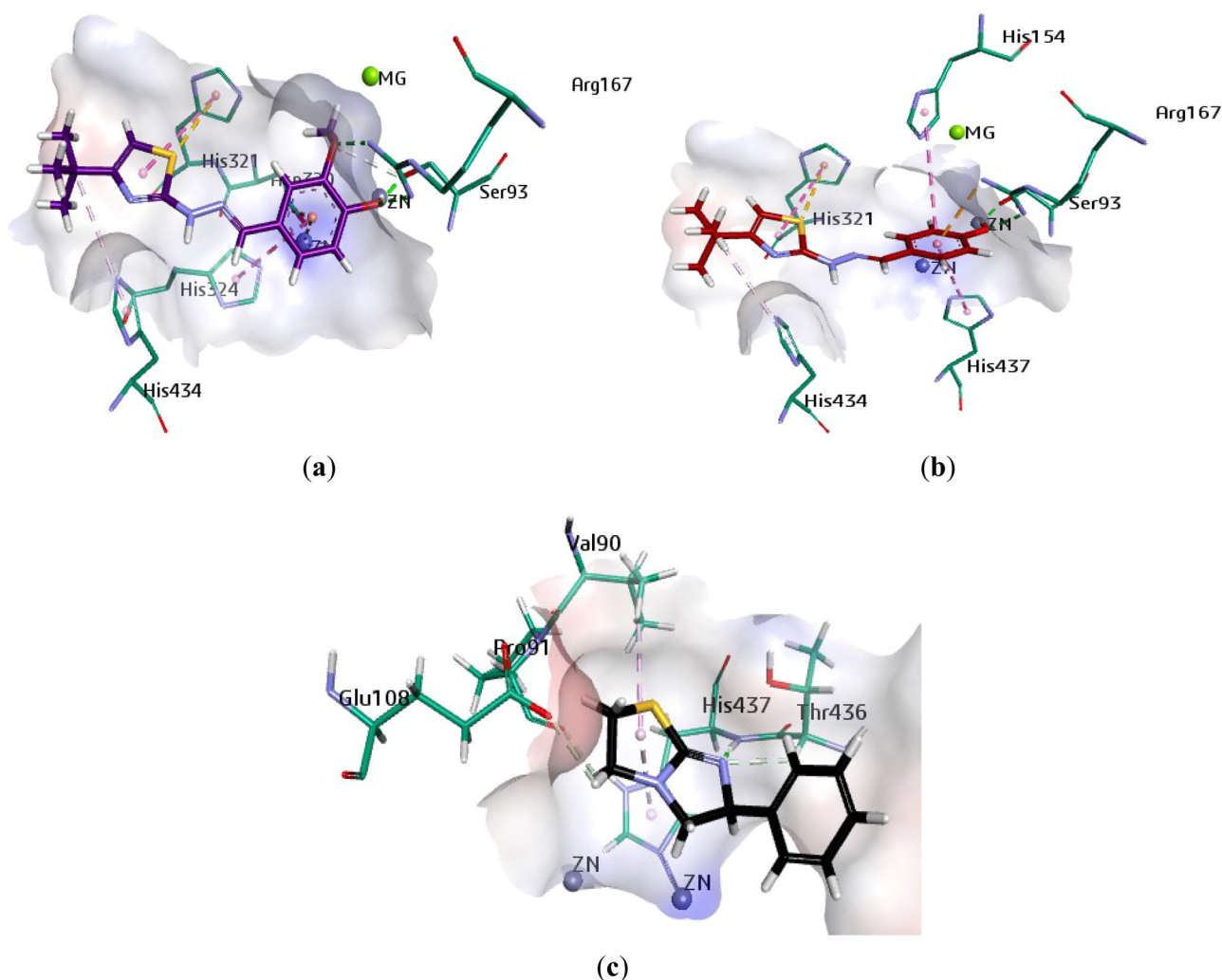


Figure 4. Plausible binding modes of compounds **5e** (a); **5b** (b) and **Levamisole** (c) inside tissue non-specific alkaline phosphatase model.

within the active site of IAP (Khan et al., 2015; Salar et al., 2017). Therefore, the resultant interactions of our selected active compounds are in accordance with the interaction residues and interaction linkages with already reported ones. The structure-activity relationship and the docking studies of identified potent inhibitors provide an outstanding platform for further development of alkaline phosphatase inhibitors. The results of docking studies for the selected compounds were descriptive of the *in vitro* enzyme inhibitory activity results, and the plausible binding poses elucidated the binding modes of these analogues (Figure 5).

The MD simulations undertaken for the docked pose of selective inhibitor (**5e**) bound to **h-TNAP** and **5d** to **h-IAP** reveal the stability of the ligand and target protein over the tested 20 ns time span during the computations. Molecular dynamic trajectories for the selected ligands with the respective protein were assessed in terms of the structural stability (Figure 6). In contrast, movements of the backbone in apoprotein in relation to the active site residues produced root-mean-square deviation (RMSD), plotted as a function of time, remain deviated over the simulation time. Figure 6 showed that the main binding orientations reported by **h-TNAP** + **5e**. In the presence of ligands **5e**

and **5d** within the active pocket of **h-TNAP** and **h-IAP**, respectively, the protein back bone RMSD values were comparable to that of the protein only (Figure 6). Moreover, the RMSF values of protein alone and in combination with selected ligands initially rise to small fluctuations from their initial coordinates while with inactive residues, the fluctuations were lower, however, again after residue number 380, the most of the fluctuations were noticed in both the proteins (Figure 7).

In case of radius of gyration plot for both the proteins in apo and holo form, Figure 8 showed that holo state of protein in complex with selected ligands was more stable as compared to apo form. The 4-hydroxy, 3-methoxybenzylidene moiety of **5e**, while 3,4-dimethoxybenzylidene group of **5d** are the key factors in the interaction and maintenance of overall stability in the protein-ligand complex. With the structural drift at some positions in both the proteins in apo and holo form, the overall trajectory of the enzyme + ligand complex exhibited the stability in the system. The interaction figures revealed that 4-hydroxy, 3-methoxybenzylidene moiety of **5e** in **h-TNAP** and 3,4-dimethoxybenzylidene group of **5d** in **h-IAP** played very significant role in the stabilizing of protein + ligand complex.

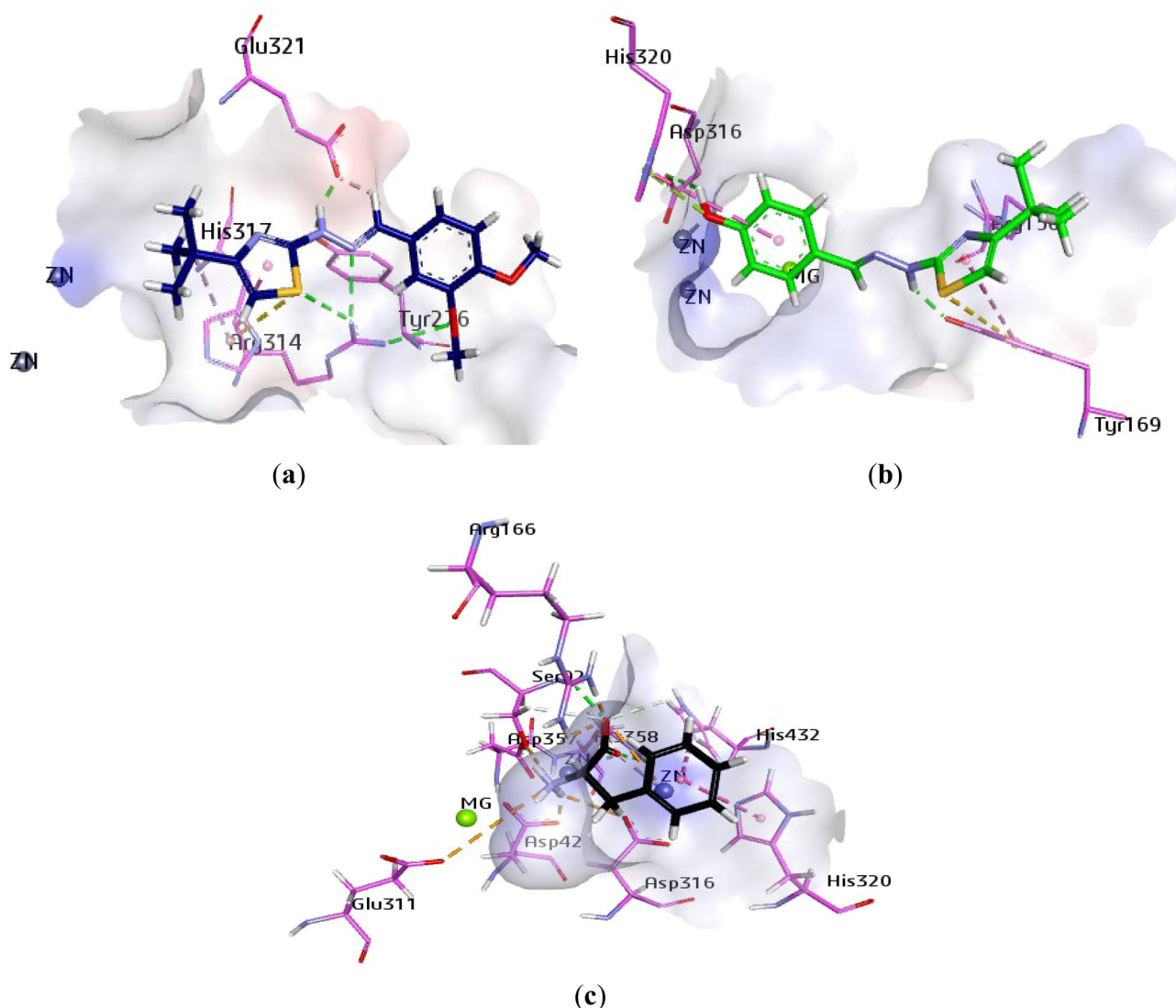


Figure 5. Plausible binding modes of compounds **5d** (a); **5b** (b) and **L-phenylalanine** (c) inside intestinal alkaline phosphatase model.

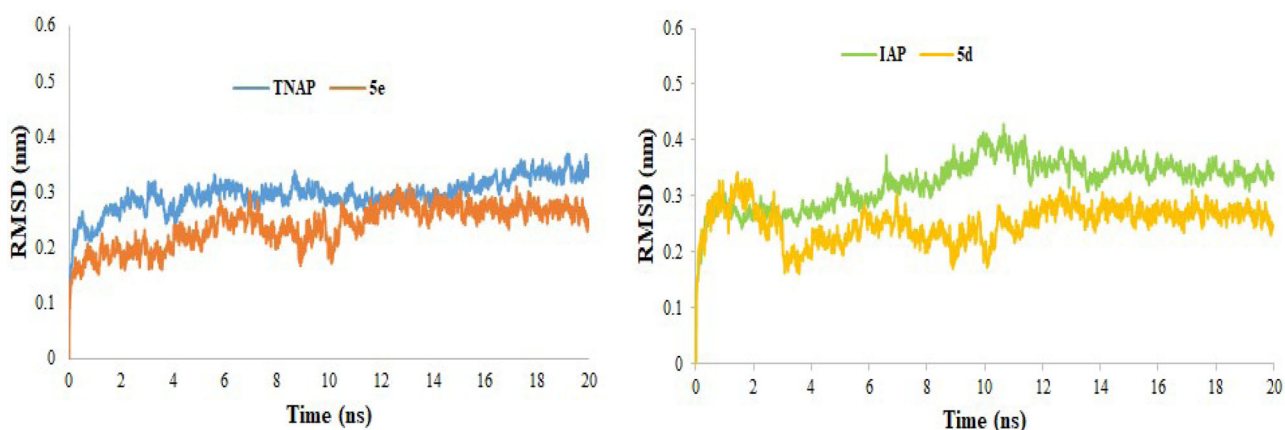


Figure 6. Root Mean Square Deviation (RMSD) of amino acid residues of *h*-TNAP and *h*-IAP protein during 20 ns MD-simulation run.

3.4. HYDE assessment of selective compounds against alkaline phosphatases (*h*-TNAP and *h*-IAP)

HYDE visual affinity of all the ligands was carried out in LeadIT (2017) software for top30 ranked docked conformers within the active site of the homology models of human *h*-

TNAP and ***h*-IAP**. The binding energy and docking score by FlexX for the all the synthetic derivatives are given in Table 3. The FlexX docking score depicted that the selective derivatives has lower energy scores as compared to non-selective inhibitors. Moreover, the binding free energies ΔG given in Table showed that the potent inhibitors exhibited higher

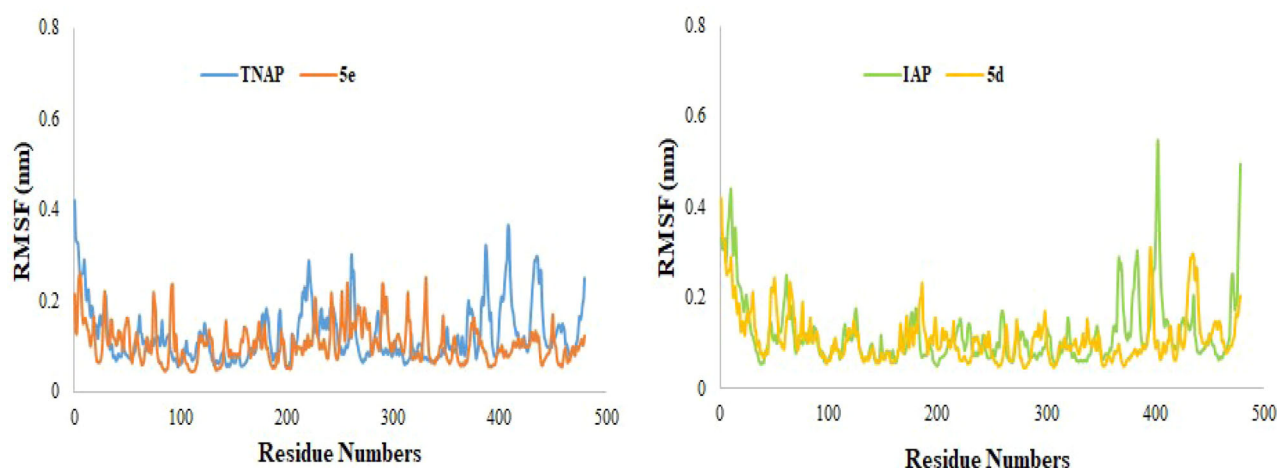


Figure 7. Root Mean Square Fluctuation (RMSF) of amino acid residues of *h*-TNAP and *h*-IAP protein during 20 ns MD-simulation run.

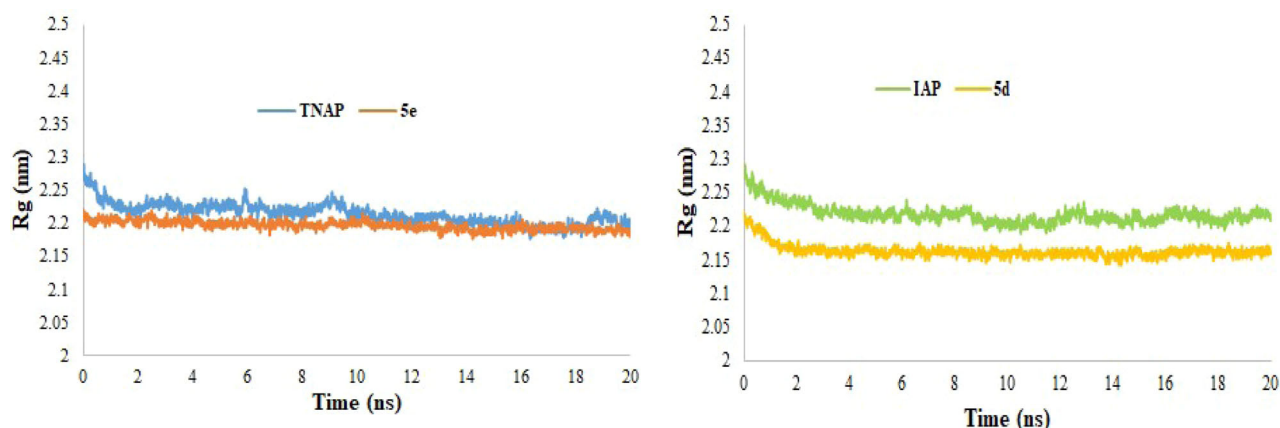


Figure 8. Radius of gyration (Rg) of amino acid residues of *h*-TNAP and *h*-IAP protein structures during 20 ns MD-simulation run.

Table 3. Docking score of the top pose of selected compounds and their ranks after HYDE visual inspection.

Compound	Docking score by FlexX for top pose (kcal mol ⁻¹)	Free energy of binding ΔG (kJ mol ⁻¹)
<i>h</i>-TNAP		
5a	-13.11	-10
5b	-16.43	-11
5c	-7.12	-2
5d	-8.99	-4
5e	-21.36	-15
5f	-8.15	-3
5g	-19.82	-7
5h	-8.35	-4
5i	-18.64	-13
<i>h</i>-IAP		
5a	-16.14	-13
5b	-17.01	-10
5c	-7.98	-2
5d	-22.31	-19
5e	-16.88	-12
5f	-8.85	-2
5g	-19.12	-18
5h	-15.67	-11
5i	-9.65	-1

affinity towards the respective target (*h*-TNAP and *h*-IAP). The compound **5e** interacts with the *h*-TNAP in a very efficient manner in comparison with **5b** and give favorable

contributions. Similarly, **5d** showed greater affinity than **5b** towards *h*-IAP. The docking scores of all the compounds revealed the similar pattern as was suggested by the *in vitro* analysis. The compounds which were inactive exhibited less docking scores, while active and potent ligands gave a significant docking scores with the significant free binding energy values.

4. Conclusions

The current research study reports the successful synthesis and characterization of 1-benzylidene-2-(4-tert-butylthiazol-2-yl) hydrazines. The compounds were evaluated to determine their inhibitory potential using alkaline phosphatases (*h*-TNAP and *h*-IAP). The screened compounds exhibited good inhibitory activity for **APs**. Compound **5e** possessed the highest inhibitory potential for *h*-TNAP with an IC₅₀ value of 1.09 ± 0.18 μM, while the compound **5d** was found to be most active against *h*-IAP with an IC₅₀ of 0.71 ± 0.02 μM. The structural elements necessary for **APs** inhibition were investigated and the most probable binding site interaction of the inhibitors with the **APs** were evaluated by molecular modelling studies. In future prospective, the investigated compounds may serve as a pharmacophore as well as lead compounds in the design and synthesis of more potent and

selective inhibitors of alkaline phosphatase. This may be the step towards medicinally important compounds for treatment of pathological dysfunctions due to APs over-expression.

Disclosure statement

The author(s) declare that they have no conflict of interests.

Funding

H.A. acknowledges an Indigenous scholarship from Higher Education Commission of Pakistan as a financial support. J.I. is thankful to the Higher Education Commission of Pakistan for the financial support through Project No.Ph-V-MG-3/Peridot/R&D/HEC/2019. J.S. received support from the Natural Sciences and Engineering Research Council of Canada (NSERC; RGPIN-2016-05867).

ORCID

Aamer Saeed  <http://orcid.org/0000-0002-7112-9296>

References

- Al-Rashida, M., Raza, R., Abbas, G., Shah, M. S., Kostakis, G. E., Lecka, J., Sévigny, J., Muddassar, M., Papatriantafyllopoulou, C., & Iqbal, J. (2013). Identification of novel chromone based sulfonamides as highly potent and selective inhibitors of alkaline phosphatases. *European Journal of Medicinal Chemistry*, 66, 438–449. <https://doi.org/10.1016/j.ejmech.2013.06.015>
- Andleeb, H., Hameed, S., Ejaz, S. A., Khan, I., Zaib, S., Lecka, J., Sévigny, J., & Iqbal, J. (2019). Probing the high potency of pyrazolyl pyrimidinetriones and thioxypyrimidinediones as selective and efficient non-nucleotide inhibitors of recombinant human ectonucleotidases. *Bioorganic Chemistry*, 88, 102893. <https://doi.org/10.1016/j.bioorg.2019.03.067>
- Ausekle, E., Ejaz, S. A., Khan, S. U., Ehlers, P., Villinger, A., Lecka, J., Sévigny, J., Iqbal, J., & Langer, P. (2016). New one-pot synthesis of *N*-fused isoquinoline derivatives by palladium-catalyzed C-H arylation: Potent inhibitors of nucleotide pyrophosphatase-1 and -3. *Organic & Biomolecular Chemistry*, 14(48), 11402–11414. <https://doi.org/10.1039/C6OB02236G>
- Ayati, A., Emami, S., Asadipour, A., Shafiee, A., & Foroumadi, A. (2015). Recent applications of 1,3-thiazole core structure in the identification of new lead compounds and drug discovery. *European Journal of Medicinal Chemistry*, 97, 699–718. <https://doi.org/10.1016/j.ejmech.2015.04.015>
- Bergman, J. M., Coleman, P. J., Cox, C., Lindsley, G. D. C. H., Mercer, S. P., Roecker, A. J., & Whitman, D. B. (2006). Praline bis-amide orexin receptor antagonists (PCT Int Appl, WO 2006127550). <https://doi.org/10.1016/j.ejmech.2015.04.015>
- Bhatti, H. A., Khatoon, M., Al-Rashida, M., Bano, H., Iqbal, N., Yousuf, S., Khan, K. M., Hameed, A., & Iqbal, J. (2017). Facile dimethyl amino group triggered cyclic sulfonamides synthesis and evaluation as alkaline phosphatase inhibitors. *Bioorganic Chemistry*, 71, 10–18. <https://doi.org/10.1016/j.bioorg.2017.01.008>
- Bisel, P., Al-Momani, L., & Müller, M. (2008). The tert-butyl group in chemistry and biology. *Organic & Biomolecular Chemistry*, 6(15), 2655–2665. <https://doi.org/10.1039/B800083B>
- Black, C., Deschenes, D., Gagnon, M., LaChance, N., LeBlanc, Y., Leger, S., Li, C. S., & Oball, R. M. (2009). Heteroaromatic compounds as inhibitors of stearyl-coenzyme a delta-9 desaturase (U.S. Patent Application 11/988, 192).
- Bradford, M. M. (1976). A rapid and sensitive method for the quantitation of microgram quantities of protein utilizing the principle of protein-dye binding. *Analytical Biochemistry*, 72(1–2), 248–254. [https://doi.org/10.1016/0003-2697\(76\)90527-3](https://doi.org/10.1016/0003-2697(76)90527-3)
- Braga, S. F. P., Fonseca, N. C., Ramos, J. P., Souza-Fagundes, E. M. D., & Oliveira, R. B. D. (2016). Synthesis and cytotoxicity evaluation of thio-semicarbazones and their thiazole derivatives. *Brazilian Journal of Pharmaceutical Sciences*, 52(2), 299–308. <https://doi.org/10.1590/S1984-82502016000200008>
- Chang, L., Duy, D. L., Mébarek, S., Popowycz, F., Pellet-Rostaing, S., Lemaire, M., & Buchet, R. (2011). Synthesis and evaluation of thio-phenyl derivatives as inhibitors of alkaline phosphatase. *Bioorganic & Medicinal Chemistry Letters*, 21(8), 2297–2301. <https://doi.org/10.1016/j.bmcl.2011.02.089>
- Dassault Systèmes Biovia. (2016). *Discovery studio modeling environment*. Dassault Systèmes.
- Ferreira, R. J., Ferreira, M. J. U., & dos Santos, D. J. (2012). Insights on P-glycoprotein's Efflux mechanism obtained by molecular dynamics simulations. *Journal of Chemical Theory and Computation*, 8(6), 1853–1864. <https://doi.org/10.1021/ct300083m>
- Gan, C., Zhou, L., Zhao, Z., & Wang, H. (2013). Benzothiazole Schiff-bases as potential imaging agents for β -amyloid plaques in Alzheimer's disease. *Medicinal Chemistry Research*, 22(9), 4069–4074. <https://doi.org/10.1007/s00044-012-0416-0>
- Haarhaus, M., Brandenburg, V., Kalantar-Zadeh, K., Stenvinkel, P., & Magnusson, P. (2017). Alkaline phosphatase: A novel treatment target for cardiovascular disease in CKD. *Nature Reviews. Nephrology*, 13(7), 429–442. <https://doi.org/10.1038/nrneph.2017.60>
- Henriksen, G., Hauser, A. I., Westwell, A. D., Yousefi, B. H., Schwaiger, M., Drzeza, A., & Wester, H. J. (2007). Metabolically stabilized benzothiazoles for imaging of amyloid plaques. *Journal of Medicinal Chemistry*, 50(6), 1087–1089. <https://doi.org/10.1021/jm061466g>
- Humphrey, W., Dalke, A., & Schulten, K. (1996). VMD: Visual molecular dynamics. *Journal of Molecular Graphics*, 14(1), 33–38. [https://doi.org/10.1016/0263-7855\(96\)00018-5](https://doi.org/10.1016/0263-7855(96)00018-5)
- Hutchinson, I., Jennings, S. A., Vishnuvajjala, B. R., Westwell, A. D., & Stevens, M. F. (2002). Antitumor benzothiazoles. 16. Synthesis and pharmaceutical properties of antitumor 2-(4-aminophenyl)benzothiazole amino acid prodrugs. *Journal of Medicinal Chemistry*, 45(3), 744–747. <https://doi.org/10.1021/jm011025r>
- Iqbal, J., El-Gamal, M. I., Ejaz, S. A., Lecka, J., Sévigny, J., & Oh, C. H. (2018). Tricyclic coumarin sulphonate derivatives with alkaline phosphatase inhibitory effects: *In vitro* and docking studies. *Journal of Enzyme Inhibition and Medicinal Chemistry*, 33(1), 479–484. <https://doi.org/10.1080/14756366.2018.1428193>
- Karegoudar, P., Karthikeyan, M. S., Prasad, D. J., Mahalinga, M., Holla, B. S., & Kumari, N. S. (2008). Synthesis of some novel 2,4-disubstituted thiazoles as possible antimicrobial agents. *European Journal of Medicinal Chemistry*, 43(2), 261–267. <https://doi.org/10.1080/10426500701641049>
- Keri, R. S., Patil, M. R., Patil, S. A., & Budagumpi, S. (2015). A comprehensive review in current developments of benzothiazole-based molecules in medicinal chemistry. *European Journal of Medicinal Chemistry*, 89, 207–251. <https://doi.org/10.1016/j.ejmech.2014.10.059>
- Khanfar, M. A., Affini, A., Lutsenko, K., Nikolic, K., Butini, S., & Stark, H. (2016). Multiple targeting approaches on histamine H3 receptor antagonists. *Frontiers in Neuroscience*, 10, 201. <https://doi.org/10.3389/fnins.2016.00201>
- Khan, I., Shah, S. J. A., Ejaz, S. A., Ibrar, A., Hameed, S., Lecka, J., Millán, J. L., Sévigny, J., & Iqbal, J. (2015). Investigation of quinoline-4-carboxylic acid as a highly potent scaffold for the development of alkaline phosphatase inhibitors: Synthesis, SAR analysis and molecular modelling studies. *RSC Advances*, 5(79), 64404–64413. <https://doi.org/10.1039/C5RA12455G>
- Khan, I., Zaib, S., Ibrar, A., Rama, N. H., Simpson, J., & Iqbal, J. (2014). Synthesis, crystal structure and biological evaluation of some novel 1,2,4-triazolo[3,4-b]-1,3,4-thiadiazoles and 1,2,4-triazolo[3,4-b]-1,3,4-thiadiazines. *European Journal of Medicinal Chemistry*, 78, 167–177. <https://doi.org/10.1016/j.ejmech.2014.03.046>
- Kukulski, F., Lévesque, S. A., Lavoie, E. G., Lecka, J., Bigonnesse, F., Knowles, A. F., Robson, S. C., Kirley, T. L., & Sévigny, J. (2005). Comparative hydrolysis of P2 receptor agonists by NTPDases 1,2,3

- and 8. *Purinergic Signalling*, 1(2), 193–204. <https://doi.org/10.1007/s11302-005-0383-8>
- Labute, P. (2007). *Protonate 3D: Assignment of macromolecular protonation state and geometry*. Chemical Computing Group Inc.
- Lau, C. K., Dufresne, C., Gareau, Y., Zamboni, R., Labelle, M., Young, R. N., Metters, K. M., Rochette, C., Sawyer, N., Slipetz, D. M., Charette, L., Jones, T., McAuliffe, M., McFarlane, C., & Ford-Hutchinson, A. W. (1995). Evolution of a series of non-quinoline leukotriene D4 receptor antagonist; synthesis and SAR of benzothiazoles and thiazoles substituted benzyl alcohols as potent LTD4 antagonists. *Bioorganic & Medicinal Chemistry Letters*, 5(15), 1615–1620. [https://doi.org/10.1016/0960-894X\(95\)00265-U](https://doi.org/10.1016/0960-894X(95)00265-U)
- Ramos-Inza, S., Aydillo, C., Sanmartín, C., & Plano, D. (2019). Thiazole moiety: An interesting scaffold for developing new antitumoral compounds. In *Heterocycles-synthesis and biological activities*. IntechOpen. <https://doi.org/10.5772/intechopen.8274>
- Chhabria, M. T., Patel, S., Modi, P., & Brahmshatriya, P. S. (2016). Thiazole: A review on chemistry, synthesis and therapeutic importance of its derivatives. *Current Topics in Medicinal Chemistry*, 16(26), 2841–2862. <https://doi.org/10.2174/1568026616666160506130731>
- LeadIT. (2017). *LeadIT* (Version 2.3.2). BioSolveIT GmbH. www.biosolveit.de/LeadIT
- Mathew, B., Haridas, A., Ucar, G., Baysal, I., Adeniyi, A. A., Soliman, M. E., Joy, M., Mathew, G. E., Lakshmanan, B., & Jayaprakash, V. (2016). Exploration of chlorinated thienyl chalcones: A new class of monoamine oxidase-B inhibitors. *International Journal of Biological Macromolecules*, 91, 680–695. <https://doi.org/10.1016/j.ijbiomac.2016.05.110>
- Maradiya, H. R., & Patel, V. S. (2003). Synthesis and application of disperse dyes based on 2-aminothiazole derivatives. *Chemistry of Heterocyclic Compounds*, 39(3), 357–363. <https://doi.org/10.1023/A:1023923012>
- Miliutina, M., Ejaz, S. A., Khan, S. U., Iaroshenko, V. O., Villinger, A., Iqbal, J., & Langer, P. (2017). Synthesis, alkaline phosphatase inhibition studies and molecular docking of novel derivatives of 4-quinolones. *European Journal of Medicinal Chemistry*, 126, 408–420. <https://doi.org/10.1016/j.ejmech.2016.11.036>
- Millán, J. L. (2006). Alkaline phosphatases: Structure, substrate specificity and functional relatedness to other members of a large superfamily of enzymes. *Purinergic Signalling*, 2(2), 335–341. <https://doi.org/10.1007/s11302-005-5435-6>
- Mishra, C. B., Kumari, S., & Tiwari, M. (2015). Thiazole: A promising heterocycle for the development of potent CNS active agents. *European Journal of Medicinal Chemistry*, 92, 1–34. <https://doi.org/10.1016/j.ejmech.2014.12.031>
- MOE. (2016). *Molecular Operating Environment* (Version 2016.01). Chemical Computing Group (CCG). http://www.chemcomp.com/MOEMolecular_Operating_Environment.htm
- Özgeriş, B., Göksu, S., Polat Köse, L., Gülçin, İ., Salmas, R. E., Durdagi, S., Tümer, F., & Supuran, C. T. (2016). Acetylcholinesterase and carbonic anhydrase inhibitory properties of novel urea and sulfamide derivatives incorporating dopaminergic 2-aminotetralin scaffolds. *Bioorganic & Medicinal Chemistry*, 24(10), 2318–2329. <https://doi.org/10.1016/j.bmc.2016.04.002>
- Ravish, I., & Raghav, N. (2016). Synthesis, pharmacological evaluation and molecular docking of some pyrimidinyl hydrazones. *Biochemistry and Analytical Biochemistry*, 5(253), 2161–1009. <https://doi.org/10.4172/2161-1009.1000253>
- Reddy, V. M., & Reddy, K. R. (2010). Synthesis and antimicrobial activity of some novel 4-(1H-benz[d]imidazol-2-yl)-1,3-thiazol-2-amines. *Chemical and Pharmaceutical Bulletin*, 58(7), 953–956. <https://doi.org/10.1248/cpb.58.953>
- Saeed, A., & Mumtaz, A. (2017). Novel isochroman-triazoles and thiadiazole hybrids: Design, synthesis and antimicrobial activity. *Journal of Saudi Chemical Society*, 21(2), 186–192. <https://doi.org/10.1016/j.jscs.2015.04.004>
- Salar, U., Khan, K. M., Iqbal, J., Ejaz, S. A., Hameed, A., Al-Rashida, M., Perveen, S., & Tahir, M. N. (2017). Coumarin sulfonates: New alkaline phosphatase inhibitors; in vitro and in silico studies. *European Journal of Medicinal Chemistry*, 131, 29–47. <https://doi.org/10.1016/j.ejmech.2017.03.003>
- Sergienko, E. A., & Millán, J. L. (2010). High-throughput screening of tissue-nonspecific alkaline phosphatase for identification of effectors with diverse modes of action. *Nature Protocols*, 5(8), 1431–1439. <https://doi.org/10.1038/nprot.2010.86>
- Schneider, N., Lange, G., Hindle, S., Klein, R., & Rarey, M. (2013). A consistent description of hydrogen bond and dehydration energies in protein-ligand complexes: methods behind the HYDE scoring function. *Journal of Computer-Aided Molecular Design*, 27(1), 15–29. <https://doi.org/10.1007/s10822-012-9626-2>
- Schüttelkopf, A. W., & van Aalten, D. M. F. (2004). PRODRG: A tool for high-throughput crystallography of protein-ligand complexes. *Acta Crystallographica Section D Biological Crystallography*, 60(8), 1355–1363. <https://doi.org/10.1107/S0907444904011679>
- Sharma, U., Pal, D., & Prasad, R. (2014). Alkaline phosphatase: An overview. *Indian Journal of Clinical Biochemistry: IJCB*, 29(3), 269–278. <https://doi.org/10.1007/s12291-013-0408-y>
- Siddiqui, N., Arshad, M. F., Ahsan, W., & Alam, M. S. (2009). Thiazoles: A valuable insight into the recent advances and biological activities. *International Journal of Pharmaceutical Sciences and Drug Research*, 1(3), 136–143.
- Turner, P. (2005). *XMGRACE* (Version 5.1.19). Center for Coastal and Land-Margin Research, Oregon Graduate Institute of Science and Technology.
- Wang, X., Sarris, K., Kage, K., Zhang, D., Brown, S. P., Kolasa, T., Surowy, C., El Kouhen, O. F., Muchmore, S. W., Brioni, J. D., & Stewart, A. O. (2009). Synthesis and evaluation of benzothiazole-based analogues as novel, potent, and selective fatty acid amide hydrolase inhibitors. *Journal of Medicinal Chemistry*, 52(1), 170–180. <https://doi.org/10.1021/jm801042a>